ABSTRACT

TRIPATTHARANAN, TAWEEWAT. Effect of Different Forming Regimes on Retention Aid Programs (PPJ Studies). (Under the direction of Martin Allen Hubbe.)

A new design of equipment called the Positive Pulse Jar (PPJ) was introduced in this study in order to compare the responses of different retention aid systems to hydrodynamic shear forces resulting from different idealized forming regimes. The major advantage of this equipment for this kind of study is the ability to simulate different forming regimes such as simple filtration, pulsation at different frequencies and amplitudes, uniform-shear forming, and a procedure corresponding to the Britt Jar method. Results showed that pulsations could increase the uniformity of paper, not only in the x-y direction, but also in some cases in the z direction as well. Under the conditions that were used for testing, a dual-polymer bridging system showed the greatest improvement in fine particle retention but this effect could be reduced by the application of hydrodynamic shear before dewatering. Following the application of high level of hydrodynamic shear, charge neutralization didn't show fully reversibility, and it was the least effective retention aid system compared with the other systems. Effects of new-designed cone rotor were also studied; making it possible to explore effects due to a well characterized average shear stress throughout the sample volume. For future studies, suggestions have been made to increase the usefulness of the PPJ as a tool in predicting the performance of new retention aid system under different forming conditions.

EFFECT OF DIFFERENT FORMING REGIMES ON RETENTION AID PROGRAMS (PPJ STUDIES)

by
TAWEEWAT TRIPATTHARANAN

A thesis submitted to the Graduate Faculty of
North Carolina State University
in partial fulfillment of the
requirements for the Degree of
Master of Science

WOOD AND PAPER SCIENCE

Raleigh
2003

APPROVED BY

_____ _____

_____
Chair of Advisory Committee

BIOGRAPHY

The author was born on June 27, 1972 in Bangkok, Thailand. He received his B.Eng degree in chemical engineering in 1995 from Kasetsart University, Bangkok, Thailand. He then worked for the Siam Pulp and Paper Public Company in Thailand as a process and product-development engineer. In August 2001, he began his graduate work on his M.S. degree in the Department of Wood and Paper Science of N.C. State University.

The author was married to the former Miss Punnee Nirattisayangkul in 1999.

ACKNOWLEDGEMENTS

The author wishes to express his deepest appreciation to all the people who have helped him during his study at North Carolina State University.

Special thanks and gratitude are extended to Dr. Martin A. Hubbe, the chairman of the advisory committee, for his invaluable guidance and support. Without him, this work would not have been possible. The guidance and constructive suggestions from the other committee members, Dr John A. Heitmann and Dr. Richard A. Venditti, are also deeply appreciated.

Finally, the author wishes to thank his family members, especially his wife, Punnee Tripattharanan, whose moral support and occasional push have bolstered him through this endeavor. This work is also dedicated to his daughter.

TABLE OF CONTENTS

Page

LIST OF TABLES

LIST OF FIGURES

Page

Page

1. GENERAL INTRODUCTION

Removal of water is considered to be one of the most important processes in the manufacturing of paper. Papermaking is basically a filtration process. The paper machine wire can be regarded as a continuous filter on which a fraction of the solids in the stock is retained. During paper forming, most of the water is removed by gravity drainage, application of vacuum, inertial effects, and pressing. It is known that not only unbound, external free water, but also fine particles such as fiber fines, filler, and other chemicals have been removed during the dewatering process. This loss of fine materials can lead to a decrease in both paper quality and productivity. It was discovered in the mid 1900's that certain chemical substances called retention aids could be used to increase the retention of material, especially fines and filler particles. At the same time, these chemicals also can accelerate drainage and subsequently lower dryer steam consumption. This was confirmed by author who found that an increase in solids content of a paper web is helpful in reduction of drying load and increase in productivity (1).

In the last few decades, scientists have developed many retention aid programs to respond to the needs for increased paper quality and production efficiency. At the same time there has been a need for suitable laboratory test procedures to evaluate the efficiencies and understand the mechanisms of different chemical programs. Between about 1969 and the present, paper technologists also have developed many test devices and procedures capable of predicting the effects of chemical additives on first-pass retention efficiency (2-5), and rates of dewatering (6-12).

Although modern paper machines have been designed to run at high speed, most of the laboratory devices cited above involve relatively slow dewatering rates. This difference makes conventional laboratory equipment and the slow pilot paper machines appear unrealistic. There have been many attempts in simulating and characterizing the drainage performance in different kinds of forming regimes (3-10). For instance, certain laboratory methods to be discussed in a later section are designed to emulate the effects of hydrodynamic shear in the approach flow to a paper machine headbox (12), the effects of hydrofoils (4-5), and the effects of vacuum boxes (7-10). An idealized forming regime known as "simple filtration" is known to occur during dewatering of an unstirred fiber slurry through a screen, as in the case of handsheet formation (11). By contrast, the pulsating flow as a wet web passes over hydrofoils can limit the tendency for a wet web to become dense, so that the dewatering process more closely resembles an idealized process of "thickening." The laboratory tools that have been developed provide a picture of what can be happening at the wet-end section. In this thesis, a new apparatus called a "Positive Pulsation Jar (PPJ)" was proposed as another choice in study of retention and drainage performance. This is the first device, since the 1960's, that allows the user to quantify not only the frequency, but also the velocity amplitudes of the flow pulsations. The scope of this study mainly focused on the validity of this equipment and the uses of this equipment in analysis of performance of major retention aid programs on various types of forming regimes.

2. RESEARCH OBJECTIVES

Laboratory equipment for drainage and retention testing has been introduced in the pulp and paper industry in the last few decades. The Britt Dynamic Drainage Jar, Water Release Analyzer, Dynamic Drainage Analyzer (DDA), G/W drainage analysis system and Moving Belt Drainage Tester (MBDT) are some interesting examples of this kind of development. However, there is no apparatus that can simulate what really happens on the forming part of a paper machine perfectly due to detrimental aspects of each device. In this project, a Positive Pulse Jar (PPJ) was introduced as another choice in simulating the drainage process happening on the paper machine. The major advantage of the PPJ is the variety of simulated forming regimes such as simple filtration, pulsation drainage and shear dewatering that can be found in the drainage process. Retention and drainage aids have been used in the process of papermaking for many years. The phenomena related to these retention aid systems were mainly attributed to their structure and the interaction of these chemicals with fibrous materials. Most of the past research mainly emphasized the effect of retention aids in only one specific drainage regime. No previous analysis of retention aid chemicals has been studied under three major different types of forming regimes since the PPJ has just been introduced.

The primary focus of this project was to develop a drainage and retention tester and prove the validity of this new equipment by performing some experiments related to retention and drainage aid programs used frequently in papermaking.

It is also proposed that major types of retention and drainage aid programs differ in their responses to different idealized forming regimes. Such differences can be illuminated by use of this new device under contrasting conditions such as simple filtration, idealized pulsation and uniform shear effect above the screen. It is further proposed that the differences in dewatering performance under differing hydrodynamic regimes can be understood in terms of such mechanisms as charge neutralization, single polymer bridges, dual polymer bridges and charged patches. The following questions constitute specific goals of the study:

1. Do retention and drainage aid systems differ in their responses to different flow regimes during dewatering?
2. Do pulsation effects and different levels of applied shear before mat forming destroy bridging mechanisms and can such effects still be observed after subsequent mat formation in the presence or absence of either oriented shear above the forming fabric or pulsating flow through the fabric?
3. Can charge neutralization and charge patch systems show "reversible" behavior when the fiber mats are formed in the presence of either pulsations or oriented shear above the forming fabric?

3. BACKGROUND

3.1 Water in the wet mat

Normally the water contained in the stock as it leaves the headbox falls into three categories (13):

- “Free water, which is held within the sheet in interstices and capillaries between fibers and fines
- “Sorbed or freezing bound water, which is tightly bound to fiber surfaces by hydrogen bonds
- “Bonded or non freezing bound water, which is part of the chemical or crystalline structure of the fiber”

The water in the wet web is removed during different phases of papermaking. Most of the free water in a paper web can be removed in the drainage, vacuum and pressing zones. The rest of water is understood to be held in very small capillary spaces either within fibers or between them. Such water can be removed only in the dryer section (14).

3.2 Sheet-forming and dewatering equipment on a paper machine

Generally, the sheet-forming process or dewatering process starts when the pulp stock coming out from the headbox impinges upon the wire of the paper machine. The words "dewatering" or "drainage" denote the movement of water out from the wet web during sheet formation. The solids level of stock in the sheet-forming process usually increases from a range of about 0.3 to 1% in the headbox to about 22 to 25% in the same wet web by the time it reaches the end of the forming section. In detail, the solids level of the stock from the headbox passing the last suction box rises approximately from 0.5 to 8.0%. This means that by far the largest quantity of water is being removed in the drainage zone, roughly 94% of the total mass (13). Sub-processes occurring within this zone include rapid drainage, the generation and decay of turbulence, the formation and breakdown of fiber networks, retention and transport of fine particles in the mat, and effects resulting from hydrodynamic shear force between the mat and the free suspension.

After that, the wet mat passes over the suction boxes to the vacuum zone, and the solid level of the web will increase to about 22%. The water removed in this second zone has been estimated to be only about 6% of the initial mass of water (13).

During formation of a conventional handsheet in the laboratory, the dewatering process proceeds mainly by the mechanism of filtration. The fibers are free to move independently and they build up in the form of discrete layers. The same filtration mechanism also is believed to be a dominant mechanism during most conventional sheet forming operations on paper machines.

Another effect called thickening occurs only if the fiber slurry is disrupted by the turbulence effect during wet web formation on the paper machine (Figure 1). An idealized thickening process is one in which the fiber slurry dewaters without a filtration layer building up on the wire. The fiber and fine materials in the pulsation mode don't move as freely as in the case of simple filtration. So, we would expect layer formation of fibers in the mat in the simple filtration mechanism that may not be found in pulsation. Though pure thickening is not expected, it is reasonable to use the term thickening when describing hydrodynamic effects that cause a wet web to remain more uniform in z-directional density during the forming process.

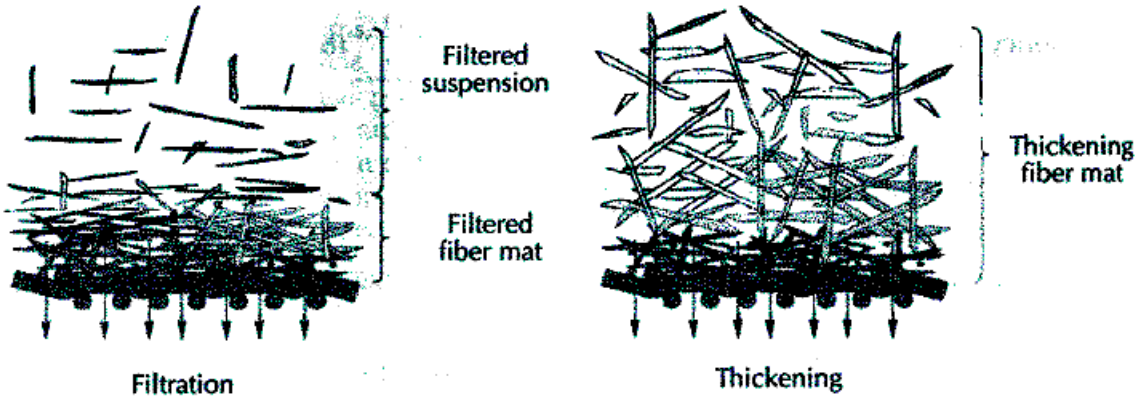

Figure 1 Difference between filtration and thickening (15)

To understand the significance of both the filtration and the thickening modes of paper formation, it is worth reviewing some of the key sub-processes that occur on an industrial-scale paper machine. One major category of paper machine forming section used nowadays is the Fourdrinier. The drainage zone on this type of paper machine can be mainly divided into two zones, the forming zone and the suction zone (Figure 2). Generally, the forces that cause drainage to take place can include gravity, the effects of vacuum boxes, vacuum at the couch roll, and applied pressure, as in the case of wet-pressing. In this case, dilution is a powerful mechanism for dispersion, but the level required to completely eliminate flocking on a paper machine is not feasible. Additional dispersion must be generated during drainage by turbulence, including effects of drainage elements below the forming fabric. That is why a wire part of a Fourdrinier paper machine has various elements between the headbox and the press section.

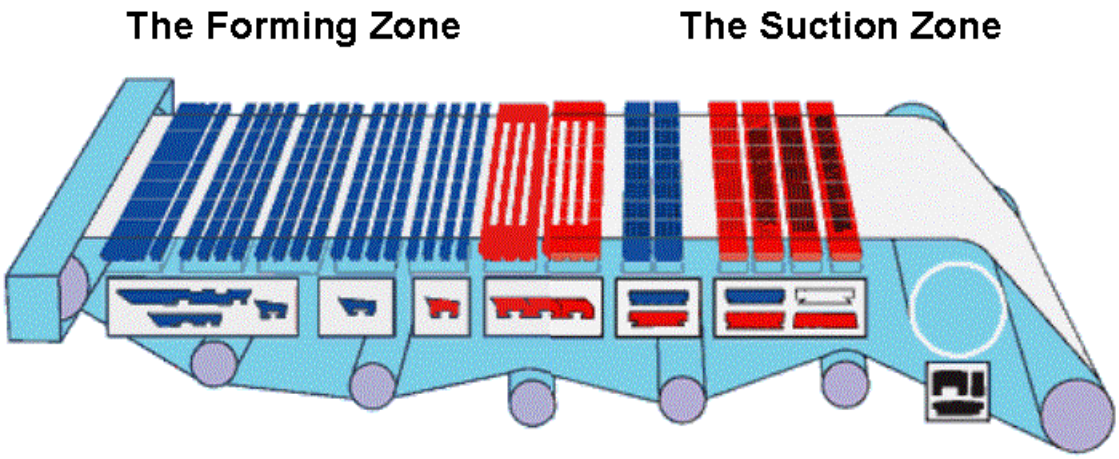

Figure 2 Two main dewatering zones on a Fourdrinier paper machine (16)

Two main rolls, a breast roll and a couch roll, support the forming fabric and promote water removal. The breast roll usually has a smooth and hard surface, but the couch roll has a perforated surface connecting to a vacuum box inside. Next to the breast roll, the first static element under the wire is the forming board. The forming board is a rigid bar supporting the wire at the point of jet impingement. Another function of the forming board is to prevent excessive initial drainage. It is reasonable to expect that such a strategy also might limit the amount of fines and filler particles that are washed out of the sheet during the initial moments of its formation.

The first suction phenomenon occurs when the wire passes over either rotating table rolls or stationary hydrofoils. A pressure pulse and a vacuum pulse are created simultaneously between the wire and the roll. The table rolls are not widely used nowadays due to the limitation in paper machine speed. Another disadvantage of table rolls is that they can

create bubbles during drainage. For this reason the elimination of table rolls can reduce the air content in the web (17).

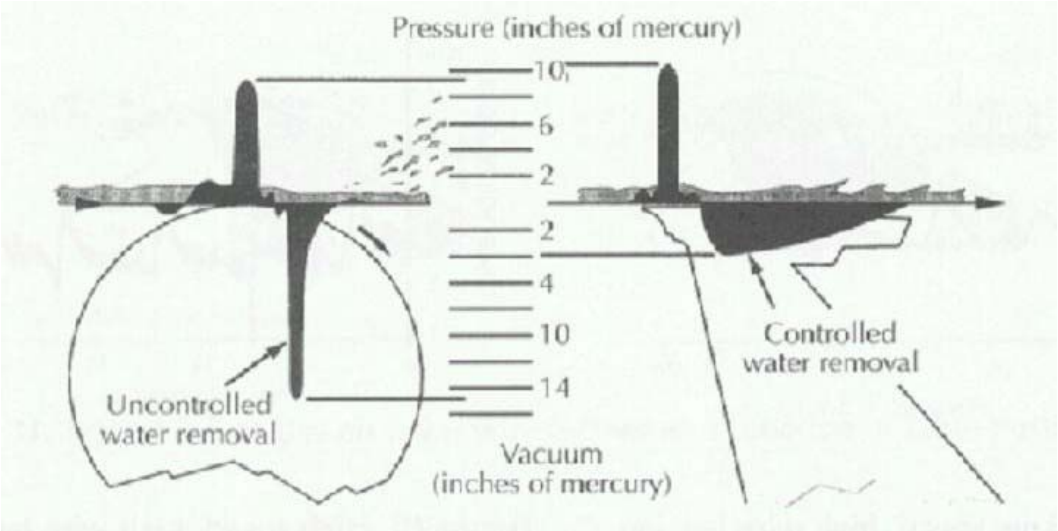

Figure 3 Difference between the pressure/vacuum pulses for both table roll and hydrofoil (15)

The next drainage element in a modern Fourdrinier forming process is a hydrofoil. The difference between table rolls and hydrofoils in flow characteristic is illustrated in Figure 3. A pressure pulse is also created along with the suction occurrence. The shape and angle of the hydrofoil are used to control the drainage characteristics (Figure 4). The pressure pulse amplitude is controlled by the foil shape. Foil spacing and paper machine speeds are used to control the pulse frequency (17). Bell (18) found that a higher pulse frequency can create better formation of paper. He also suggested that micro-turbulence action is preferential to stock jump action in formation improvement. The suction of table rolls and hydrofoils can produce a washing effect. A large proportion of fiber fines and filler can be removed from the wire side by this action. This washing process tends to create an unevenness of fines and filler in the z direction.

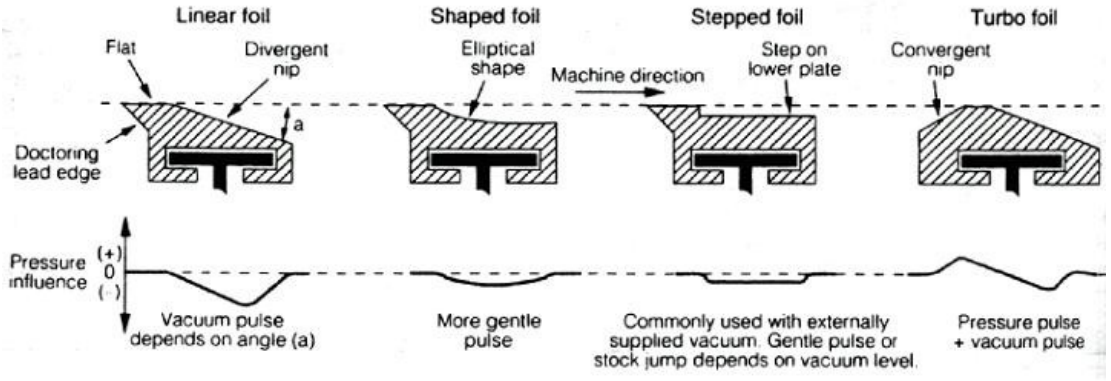

Figure 4 Hydrofoil shapes and associated pulse actions (17)

The pulsations created by table rolls or foils also change the drainage mechanism. The pure filtration mechanism is changed to be a combination of filtration and thickening (19). Parker (20) described the sheet forming process as a balance between oriented shear and turbulence patterns. He proposed that both oriented shear and turbulence play significant roles during drainage of the wet mat. The turbulence will prevent the development of a dense, relatively impermeable mat of fibers adjacent to the forming fabric (sealing), thus keeping the sheet open for drainage. Oriented shear is expected to influence the network structure by dispersing the fibers into direction of the major force (Figure 5).

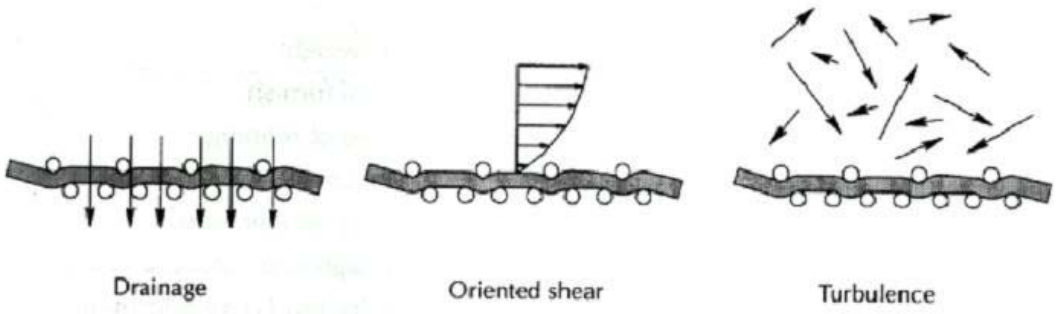

Figure 5 Different shear patterns within a fluid suspension on a wire of a Fourdrinier paper machine (19)

Further down the hydrofoil, a series of vacuum-assisted elements are used to remove the rest of water. These are ranged from low vacuum (wet boxes) to high vacuum (couch roll). The low vacuum foil or "wet boxes" are initially used to sustain the moderately high drainage rates. Next, the papermaker uses high vacuum "flat boxes" or "dry boxes." A high-vacuum flat box is used to promote dewatering of the air and water mixture. The last dewatering element in a typical forming section is a suction couch roll. The detail of couch roll is briefly explained at the beginning of this part.

3.3 Mechanisms of dewatering

Filtration theory

Generally, the filtration processes can be divided into two main categories, in-depth filtration and surface filtration (21). The term in-depth filtration, or volume filtration, denotes a filtration process in which suspended particles enter the filter media and become trapped in the porous structure. As the filtration proceeds, the permeability of the media decreases as the filter becomes increasingly filled up with material. In surface filtration, or cake filtration, the suspended particles are stopped at the surface of the filter, and they build up a layer, which is often called a cake. The cake itself may serve as an

additional in-depth filter medium and increases in filtration efficiency by trapping yet smaller particles. As a result, the resistance to flow increases with the increasing thickness of the cake (21).

Of the two models considered here, papermaking more closely conforms to cake filtration. The forming fabric can act as a filter medium during dewatering. Other sub-processes occurring during paper formation also should be mentioned in order to provide a more complete picture. For instance, Wahlstrom has suggested that fiber/fiber collisions and fiber/wire collisions influence the retention within the web (15). Recently there has been a change in focus of research, involving analysis of specific filtration resistance (SFR). Research has shown that, as the pressure differential across a wet web of paper is increased, the specific filtration resistance increases. By contrast, turbulence seems to decrease the specific filtration resistance (14).

Principle of cake filtration (22)

Cake filtration can be described as a process in which the liquid passes through two resistances in series. The first of these resistances consists of the cake itself; the second is due to the filter medium. The filter-medium resistance is expected to be important only during the early stages of cake filtration. The cake resistance is defined to be zero at the start of the process and to increase as the cake builds up.

The overall pressure drop as a function of time can be taken as the sum of the pressure drops over medium and cake. If one defines P_a as the inlet pressure, P_b as the outlet

pressure and P' as the pressure at the boundary between cake and medium, then it follows that

$$\Delta P = P_a - P_b = (P_a - P') + (P' - P_b) = \Delta P_c + \Delta P_m \quad (1)$$

where ΔP = overall pressure drop

ΔP_c = pressure drop over cake

ΔP_m = pressure drop over medium

Furthermore, some of the terms can be related to physical variables, leading to the following useful expression:

and $$\Delta P = \Delta P_c + \Delta P_m = \mu u / g_c \, (m_c \alpha / A + R_m) \quad (2)$$

μ = viscosity of the filtrate

u = linear velocity of the filtrate

g_c = Newton's law proportionality factor

m_c = total mass of solids in the cake

α = specific cake resistance

A = filter area (measured perpendicularly to the direction of flow)

R_m = filter-medium resistance

Equation 2 shows the pressure difference as a function of the filter-medium resistance (R_m). Normally the filter-medium resistance is expected to vary with pressure difference and with the age and cleanliness of the filter medium. However, it also is expected that the term corresponding to the filter medium will become less significant as the cake builds up further. Typically the value of that term is assumed to be constant during filtration. Technologists can determine its magnitude from experimental data.

The specific cake resistance, α, in equation (2) is defined by the equation (3).

$$\alpha = \Delta P_c A g_c / \mu u m_c \quad (3)$$

In a compressible cake, α depends on the location within the cake. The value of α may depend on the applied pressure difference, and the passage of time. In practice, variations of α with time and location are assumed to be insignificant or variations are ignored in order to simplify the analysis. An average value is obtained experimentally for the material to be filtered, using equation (3). Sometimes runs are carried out at different applied pressures so that α can be plotted as a function of pressure difference.

Finally, it is worth noting that the cake resistance is a function of ΔP_c rather than of ΔP. However, once filtration has proceeded forward, even to a moderate degree, it is to be expected that ΔP_m will become small in comparison with ΔP_c. In such a case specific cake resistance can be considered as a function mainly of ΔP.

Darcy's law and Kozeny-Carman equation

Darcy's law (11, 22)

For a given packed powder bed system it has been observed that the steady state flow rate usually is directly proportional to the pressure drop of the fluid. Such a system can be considered according to Darcy's law. This law can also be applied to other porous media such as filter media. The following equation is assumed to be applicable to cases involving laminar flow of Newtonian fluid.

$$Q = (k/\mu)\ (A\Delta P/L) \quad (4)$$

Q = flow rate of drainage

k = permeability constant, depending on the porous medium and the fluid viscosity.

μ = shear viscosity of the fluid

A = cross sectional area of cake

ΔP = overall pressure drop

L = cake height or cake thickness

Kozeny-Carman equation (23)

The Kozeny-Carman equation is a development of Darcy's law (11). It is widely known that the Kozeny-Carman equation shows the relationship between the rate of drainage and the packed bed characteristics (cake). It is also suitably applied in a range of laminar flow and is used when the Reynolds number is less than about 1.0. The Kozeny-Carman equation shows a quantitative relationship between permeability and porosity (24).

$$Q = (1\text{-}C)^3/K\mu S^2C^2 \qquad (5)$$

Q = flow rate of drainage

C = volume fraction solids in the cake

K = volume permeability coefficient or permeability constant, depending on the porous medium and the fluid viscosity.

μ = viscosity of the fluid

S = specific surface area of cake

3.4 Factors influencing drainage and retention (13,14,15,19)

To provide context for some of the discussion that will come later, it is worth considering some of the other paper machine variables that are expected to have some influence on either fine-particle retention or rates of dewatering.

Stock temperature: An increase in the temperature of the stock reduces the stock viscosity and thus facilitates drainage.

Surfactants: Surfactants can increase dewatering rates but also can cause problems with foaming, retention, sizing, and possibly strength.

Air in stock or entrained air: Entrained air is expected to fill the narrow spaces between fibers or other particles and retards the flow of draining water.

Fiber fines content: Fiber fines interact strongly with water and have large amounts of associated water. Following the Kozeny-Carman equation, increased surface area of the swollen fiber fines tends to increase resistance to flow or drainage (23). Fiber fines also tend to accumulate to a disproportionate degree under a pure filtration mechanism. They block the available pore area for drainage (Choke point model) (25).

Filler content: Fillers can have two, competing, effects. First, fillers do not interact with and absorb water as strongly as fibers do, and this use of fillers promotes drainage. Drainage is more efficiently improved by coarse, rather than fine fillers. On the other hand, fillers lodge in fiber mat pores where they can impede the free flow of water through the network.

Flocculation: Flocculation influences drainage by the collection of fines and colloidal substances to the fiber surfaces and by increasing the free volume for water removal. However, too strong flocculation can give voluminous flocs, which are very difficult to dewater.

Freeness of stock: Highly refined fibers or low CSF stock decrease the drainage rate. Refining is expected to generate fines due to removal of primary wall material from fibers and also by fiber cutting. Refining also develops fibrillation from the secondary wall, and this process tends to increase the surface area of the fiber (26). The increase in surface area from fines and fibrillation will reduce drainage due to the swelling of fiber and fines. Fines can further block the pore area for drainage. Moreover, refining increases the fiber flexibility, a change that could be expected to produce a denser mat with smaller pores. A denser will have less space for the flow of water.

Polyelectrolytes: Polyelectrolytes used for improving drainage in the forming section can actually cause less vacuum-zone drainage due to an increase in the porosity of the sheet or bad formation. Water is quickly replaced by air when air is able to leak through channels of lighter areas of the wet web (7,13).

Vacuum: Unbehend and Rowland showed that dewatering in a vacuum-assisted zone was governed by compression. The subsequent densification of the wet web is the major mechanism of water removal, since a denser web has less space for free water (27).

3.5 Some interesting retention and drainage test equipment

A number of devices have been developed for laboratory retention and drainage studies in the past few decades. They either are static type (sheet molds, drainage testers), or they are equipped to produce controllable shear level. Some types permit the simultaneous measurement of drainage rate and/or sheet properties. However, some devices have been developed to monitor the extent of flocculation (28-29). Below are some examples invented for drainage and retention evaluation.

Freeness Tester: Because of their simplicity of operation, freeness testers are the most frequently used laboratory drainage tester. It is a practically empirical test. It can also be used to measure the drainage time of a specific volume of water from a given quantity of pulp suspension. The disadvantage of using a freeness tester has been that the test is very sensitive to the quantity of fines in the wet mat. Freeness tests tend to overemphasize the effects of fine content in comparison with conditions prevailing on the paper machine (13). Other critical features in the freeness tester which differ from the dewatering on the paper machine include a lack of effect of hydrodynamic shear, fiber flocs, and pressure pulsations (12).

Application of Freeness Tester

Onabe (30) used the freeness tester as one part of a study of interfacial phenomena, using the colloid titration method. He found that there was a slight increase in freeness of the beaten pulps due to addition of flocculating agents. Sampson and Kropholler (31) presented a modified freeness apparatus for replacing the traditional freeness tester and characterized the drainage curves of the pulp.

Dynamic Drainage Analyzer (DDA): Forsberg and Bengtsson (32) proposed this equipment in 1990. It consisted of a drainage unit and a microprocessor. The microprocessor controls the time of dosage of chemicals as well as the time and speed of stirring. There was no undesirable delay time between the addition of chemicals and the drainage test, and the necessary hydrodynamic shear was maintained during the experiment. The device can be used in either static or dynamic drainage under free or vacuum-assisted conditions. The advantage of this equipment was that retention, drainage, porosity and wet web dryness were measured simultaneously from the same sample. The porosity of the sheet formed in the DDA had a good correlation with the drainage rate and the wet web dryness that also correlated with the dryness before size press fairly well.

G/W Drainage Analysis System: In 1983, Gess (33) introduced the G/W Drainage Analysis System. This equipment was mainly used to study the drainage rate under the influence of a constant flow rate of vacuum pump (volume/time). The G/W drainage graph was plotted and showed the four zones of drainage character, the wet line, the dry line, a free water area, and a pressing zone. The results showed that there was a linear correlation in drainage time between G/W system and TAPPI standard method (using a handsheet device), but it was a non-linear correlation in case of G/W drainage time and Canadian Standard Freeness. In 1993, Gess introduced another device called the Weyerhaeuser "Retention Aid Evaluation Variant" (RAEV). He studied the effect of anionic polymers and mixing time on the drainage characteristics. The drain time from RAEV was equivalent to the "B" time on the G/W test. He found that anionic PAM

slowed drainage initially but the slowing cannot be overcome by time and shear at high levels of this chemical (34).

Retention Process Analyzer (RPA): In 1992, Saharinen, Cheng, and Paulapuro (35) proposed a new laboratory device called Retention Process Analyzer (RPA). The RPA was specially designed for characterizing the influence of shear forces on retention. A single-polymer retention aid system was selected to use in their study. The high shear pulse was generated by increasing stirring speed from 500 to 1500 rpm and maintaining it for a short time (1-10 seconds). However, the "pulse" used by these authors resulted in shear parallel to the plane of the screen; this is in contrast to other devices considered in the previous work where the "pulsating flow" involves mainly a vertical component of velocity though the wire. The major conclusion from the cited study was that a high shear pulse had a slightly positive effect on retention aid effectiveness at the beginning of retention aid mixing (less than 3 seconds after retention aid mixing). When the pulse was applied later, the retention was decreased by the shear force due to deflocculation.

Turbulent Pulse Sheet Former: Persson and Osterberg (6) invented a laboratory apparatus for pulsed drainage in 1969. They used this apparatus for measuring the drainage character under the effect of pulsations perpendicular to the plane of the forming fabric. The apparatus was comprised of a pneumatic system for creating pressure pulses, a pressure transducer for measuring the value of drainage pressure, and a rotating valve for adjusting the pulse frequency. They varied the pulse frequency from 0 (constant pressure) to 100 Hz. The pressure and filtrate volume were recorded continuously and could be used in basis-weight calculations. A few experiments about basis weight, flow

velocity and drainage resistance were studied to support the validity of the equipment. The disadvantage of this apparatus was that it couldn't measure the basis weight and flow velocity directly.

Moving Belt Drainage Tester: The Moving Belt Drainage Tester (MBDT) was introduced in 1992 by Räisänen, Karrila, and Paulapuro (4-5). It was a device that simulates the conditions of drainage and pulsation that occur on the wire during papermaking. The pulsation was accomplished by the use of an endless moving belt equipped with the perforated cogs beneath the stationary wire in the sheet former of the tester. With the MBDT, the vacuum profile and pulsation frequency were adjustable to realistic levels. A pulse rate of 80 Hz yielded a filler distribution that was similar to a commercial Fourdrinier paper machine. White water can constantly be removed and measured qualitatively and quantitatively. First pass retention or wire retention can be determined while a sheet for structure analysis is being formed. The inventors also found that water removal was mainly affected due to mat compression, not air movement. Shear forces before forming affected retention (and Z-distribution), but not vacuum drainage. They concluded that at higher pulse frequency, the poorer retention occurred. These results were more dependent on the furnish characteristics than the basis weight.

Britt Dynamic Drainage Jar:

The most common tool adopted for retention studies in the laboratory is definitely the Britt Dynamic Drainage Jar, or the Britt Jar. The Britt Jar has been used extensively through out the industry as a quick, accurate and uncomplicated way of studying fines retention. It has been used by those carrying out research on polymer additives and

retention aids because of its ability to mimic performance on the paper machine, not for drainage evaluation. However, the Britt Jar can be used in conjunction with a mixing device where chemicals were added onto the stock and then transferred to a SR or CSF tester. Drainage volume or drainage time can be recorded. The Britt Dynamic Drainage Jar consists of a cylindrical container equipped with a perforated bottom plate or wire. A stirrer with an adjustable rotational speed created a turbulent condition, as required in the test. Different levels of turbulence can be simulated by varying the residence time and the speed of the stirrer to the actual level of retention on the machine. The drained filtrate can be collected within a specific time (36), for example 30 sec (37), from the initial stock (500 ml @ 0.5% consistency) (38). An alternative container with 3 vertical vanes on the inside wall increases the turbulence at a given rpm. Unfortunately, the two major disadvantages of Britt Jar are lack of filtration effect from mat formation and lack of recirculation. However, the latter can easily be addressed by using a filtrate recirculation arrangement. Operation details of the jar can be found in the Information Manual furnished with each instrument and also in TAPPI Method T 261 (37).

Applications of the DDJ and modified DDJ

The DDJ in its original format can be used in two distinct functions: fractionation applications and retention applications. At the beginning, Britt (39) used the jar in studies of the presence of stirring, using results at different stirring speeds to represent the retention on different paper machines. He and Unbehend also tested the validity of using the Britt Jar in fractionation of fine content in the paper mill (40). Avery (41) used the original type of Britt jar in evaluation the effect of alum on retention. Milliken (42) determined the fines retention by using the DDJ and compared the results with a

spectrophotometric method. Pelton, Allen, and Nugent (43) used a Britt Jar with a paper machine fabric to characterize the retention in the process. They also measured drainage times to confirm the absence of mat formation. In 1976, Unbehend (44) explained the mechanisms of “soft” and “hard” floc through the Britt Jar experiment. He also introduced a modified Britt Jar with vacuum application in 1977. The modified dynamic drainage jar called the “Water release analyzer (WRA)” was introduced officially by Britt and Unbehend in 1980 (45). They collected the filtrate that was collected in 10 sec during vacuum exposure and named the method the “10X drainage test”. They also found that over-flocculation due to dual polymers can be reduced by the mechanical dispersion technique and it will make a higher-dryness mat on the wire-part of the paper machine. Wegner, Springer, and Chandrasekaran (2) used a modified WRA with the liquid-sensing electrodes for measuring the drainage rate. Increasing polymeric additive levels increases drainage rates and retention but decreases web dryness in response to vacuum. Britt and Unbehend (8) continued using the WRA to study the effect of different vacuum levels on drainability of different furnishes in 1985. The data showed that drainability increased as the fines content decreased in the gravitational condition but maximum drainability was found at an optimum fines content in the vacuum condition. The report by Britt, Unbehend, and Shridharan (46) in 1986 also showed that fines can have a very large negative effect on dewatering in a "pure filtration" mode but have less effect in the presence of pulsation.

Inverted Cone:

Arslan et al. of the University of Maine (47) originally initiated use of an inverted cone rotor in conjunction with a jar test and used it in studying the effect of shear force on fine particle retention. The inverted cone replaced of the usual impeller and reduced the non-uniformity of shear stress in the DDJ. The authors made some comparisons of the effect of a shear force using the original impeller and the inverted cone. The results showed that the drainage rate decreased to a minimum at 750 rpm and a filter cake formed most rapidly at this speed. The results also indicated that a filter cake was not forming at high speed because of the shear field or that the filter cake that was formed had a high void fraction. The ash retentions from both stirrers were the same but the difference in fiber fines retention was large.

3.6 Major retention and drainage chemical programs

Generally speaking, all the chemicals used for retention and drainage can be classified into four fundamental mechanisms: (i) bridging, (ii) charge neutralization, (iii) charge patch interactions and (iv) microparticle system (not included in this thesis) (48).

Bridging

Bridging is a term used to describe the ability of certain dissolved polymers to agglomerate suspended particles or to cause flocculation of fiber slurries, especially in the presence of flow (49). According to the bridging single-polymer model, the polymer first adsorbs partly onto one surface, and then loops or tails become attached to a second surface. In the dual polymer model, an anionic polyelectrolyte can be a very effective bridging agent for papermaking fibers if these have been treated with a cationic material

so that there are positive sites on those surfaces. If shear forces break polymer bridges, the degradation is irreversible. Then, we can get patching or steric stabilization since the anchoring sites for the polymer at the interfaces remain occupied (50). Single Polymer bridging relates to the retention aids with a low charge density and a high molar mass. Dual Polymer bridging involves with a moderate-mass, high-charged cationic polymer and a very high mass anionic acrylamide copolymer (aPAM).

Charge Neutralization

Charge neutralization refers to a state in which the net electrical charge of particles and polyelectrolytes in aqueous solution have been canceled by the adsorption of an equal number of opposite charges (51). The main idea behind the charge neutralization model is the elimination of electrostatic double-layer repulsion between fibers and other suspended particles in the furnish. Then, Van der Waals forces will cause agglomeration (25). It makes sense to use a highly charged cationic material at a level that just balances the net surface charge of the furnish. Charge neutralization is expected to promote dewatering by allowing colloidal fines to adhere onto fiber surfaces rather than being able to block drainage channels during dewatering**.** Charge neutralization has been considered as a reversible process after the shear exposure. It was found that the typical length of time required to re-form fiber flocs after a headbox-type fiber furnish has been exposed to a high level of hydrodynamic shear is 500 milliseconds (50). Maximum rates of dewatering are sometimes associated with charge-neutralization of fibers surfaces.

Charged Patch Interactions

Highly charged cationic polyelectrolytes with molecular masses in the range of 100,000 to 2 million grams per mole are expected to interact according to a charge patch model. In principle, a non-equilibrium stage of flocculation, corresponding to the bridging mechanism may possibly be created in the system in the early stage, just after the chemical is added. High shear forces in the system cause the polymer to lie down. It is reasonable to describe the resulting pattern, in the case of small polymers, as a mosaic; large molecules would be expected to yield larger patches on the wetted surfaces of a stirred suspension. Then, positive patches attract uncovered anionic areas creating coagulation. In principle, a patch system would be expected to form strong, reversible flocs, but mosaics would be weaker. Zeta potential need not be zero in optimization of the charged patch system. Maximum performance is expected at 50% coverage (48). Charged patches are considered a reversible process, as in the case of charge neutralization. Ström and Kunnas (52) found that High mass PEI polymer was most effective for increasing the drainage rate at a relatively low dosage (*e.g*. 0.02% by mass based on dry pulp).

3.7 Charge measurements and principles

Fibrous materials and filler surfaces are generally anionic charge. The repulsive forces created by the surface charge of these particles play a role in stability of the system. To overcome these repulsive forces, chemicals that have positively charged surfaces are added to flocculate or coagulate theses particles and retain these materials on the wire of a paper machine. Charge measurement is considered an important tool in determine the

optimum dosage and control of these chemicals. Generally, surface charge analysis has been done on the following devices.

Zeta Potential

The zeta potential is defined as the average electrical potential at a hydrodynamic slip plane adjacent to a solid surface exposed to a liquid. A furnish having a zeta potential near to zero is more likely to drain well, especially if the drainage mechanism is dominated by charge neutralization or a charged patch model. Microelectrophoresis is the most common way that papermakers evaluate the zeta potential of fiber fines and fillers. Electrophoretic mobility of the particles, zeta potential of the particles, and strength of the electric field are proportional to particle velocity in microelectrophoresis test. Commercially available fiber-pad streaming potential devices often yield a nominal "zeta potential," but it is not expected to agree with results from microelectrophoresis (50).

Mobility values may be converted into zeta potentials by means of the Smoluchowski equation (25), although the experimental conditions may not always conform to the assumptions on which that equation is based.

Streaming Current

The streaming current method is one of the most widely used means of detecting the endpoint of a charge demand titration. Colloids from the sample adsorb onto a Teflon surface, and flow of water past those walls move some of the counter-ions that are outside of the shear plane, creating an electrical current or potential. During an evaluation of colloidal charge of an aqueous sample one adds an oppositely charged titrant until the signal goes to zero. In theory, this condition occurs when neutral complexes between the

titrant and components of the sample become less soluble and cover the probe surfaces. It has been found that the streaming current measurement does not necessarily reflect the exact zeta potential of suspended particles, but rather indicates whether a system is cationic or anionic. However, it has been shown, that the point of charge reversal of a suspension often does correlate with charge reversal point on the piston and cylinder surfaces when polyelectrolyte are used to change the charge in the system (50).

Streaming Potential

Streaming potential is an induced potential difference of a mat forming on the screen between the two electrodes. In details, fiber-pad streaming potential testing typically has following actions (14)

1. Form a fiber pad on a screen.
2. Flow pushes counter-ions adjacent to charged surface.
3. Measure the electrical potential difference across the pad at a known applied vacuum.

Streaming potential is related to zeta potential by factors that include the electrical conductivity, fluid viscosity, and the structure of the fiber pad. Unfortunately, laminar flow must be assumed and achieving a pad with a uniform and repeatable pore size is difficult.

4 MATERIALS AND EQUIPMENT

4.1 Stock composition

The recipe and details of stock composition were shown in Table 1.

Table 1 Furnish recipe in the experiment

Item	Amount	Description
Stock	Approx. 45% by mass	Bleached kraft pulp, refined to approximately 400 ml CSF
Extra fines	Approx. 25% by mass	Fines collected by Bauer-McNett fractionation of refined hardwood pulp through a 200-mesh screen
Filler	Approx. 30% by mass	Scalenohedral precipitated calcium carbonate filler

Fibers fraction: A moderately refined bleached kraft pulp was the main focus of this project. Hardwood bleached kraft pulp (market pulps) was soaked, dispersed and refined following TAPPI Method T200 (53) to 400 ml CSF. The fiber fraction was obtained from the fractionation process. Details of refining and fractionation can be found in the Appendix A and B of this report. When not in use, the fiber fraction slurry was kept in a 5-gallon bucket and stored in a cold room. The standard fibers fraction for all experiments was set at 45% by mass.

It is worth noting that due to the limitation of fractionation procedure, the fibers fraction slurry prepared in this experiment is not absolutely pure fiber content. With the FQA analysis, there were around 25% of fines (based on number of particle) in this fibers fraction slurry.

Fines fraction: In this work, we consider that those particles which pass a 76 μm hole size (200 mesh) are fines fraction. This fraction consists of a mixture of primary fines from the original source of wood and secondary fines from the refining process. The fines fraction slurry was prepared from the filtrate of the 400 ml CSF refined pulp passing through the Bauer-McNett fractionator. This filtrate was kept unstirred overnight to allow

sedimentation of the fines. Supernatant water (upper-level water) was removed to increase the consistency of the fines slurry for ease of storage. The fractionation procedure can be found in Appendix B.

It is worth noting that the fines fraction or extra fine ingredient was initially set at 25% by mass. Because the fiber fraction approximately has 25% fines (by number) in itself, the actual total fines amount in final prepared slurry is 73-75% (by number) with the FQA analysis. The percent of fines based on length-weighted calculation is around 27-29%.

Filler fraction: Precipitated Calcium Carbonate (PCC) was selected in this experiment as a filler component of the paper. The product was Albacar® 5970 supplied by Specialty Mineral Inc. (SMI). This product is classified as a scalenohedral type of PCC with the particle size range smaller than 2 microns. In this experiment, the filler fraction was set at approximately 30% by mass.

4.2 Major chemicals

Single Polymer Bridging Chemicals: Cationic Polyacrylamide (cPAM)

Dual Polymer Bridging Chemicals: Anionic Polyacrylamide (aPAM) and Poly-diallyldimethylammonium chloride (Poly-DADMAC)

Polyacrylamide

Acrylamide products used as retention aids typically have molecular masses in the range 5 to 20 million grams per mole. The cationic copolymers usually have no more than 5% of cationic groups (54). Cationic polyacryamides mostly have quaternary ammonium groups in cationic monomers used (25). Anionic polyacrylamides usually have a

maximum dosage level, after which point formation is no longer acceptable. For modern high molecular weight systems, this level is usually less than 0.05% on fiber weight (15).

Poly-diallyldimethylammonium chloride (Poly-DADMAC)

Poly-DADMAC is a linear homopolymer formed from a monomer that has a quaternary ammonium and two unsaturated -CH=CH_2 functionalities. The molecular weight of DADMAC is typically in the range of hundreds of thousands of grams per mole, and even up to a million for some products (55).

Charge Neutralization Chemicals: Poly-DADMAC (followed the details above)

Charge Patch Chemicals: Modified Polyethyleneimine (PEI)

Polyethyleneimine (PEI)

The monomer of PEI consists of a three-membered ring. Two corners of the molecule consist of -CH_2- linkages. The third corner is a secondary amine group, =NH. In the presence of a catalyst this monomer is converted into a highly branched polymer with about 25% primary amine groups, 50% secondary amine groups, and 25% tertiary amine groups. This product is sometimes called "pure polyethyleneimine" in order to differentiate it from certain copolymers of ethyleneimine and acrylamide. The latter mixture is copolymerized to produce so-called "modified PEI," that has a molecular mass up to about 2 million grams per mole. Pure PEI is very effective for neutralization of excess anionic colloidal charge, especially under acidic and neutral pH conditions.

Modified PEI copolymers having relatively high molecular mass can be effective for drainage (56).

An important factor affecting performance of PEI products is pH. When pH is increased from 4 to 10, the cationic charge of PEI decreases because the amine groups are not of the quaternary ammonium type (25).

The specific details of chemicals used in this thesis are included in Table 2.

Table 2 Summary of retention aids used in thesis work

Brand name	Company	Category	Mass range	MM g/mol	Charge range	Charge type
Bridging						
Single Polymer						
Percol® 455	Ciba Specialty	PAM	Medium-high	n.a.	Low	Cationic
Dual Polymer						
Alcofix® 169	Ciba Specialty	Poly-DADMAC	Low	300,000 (mass based)	High	Cationic
Floerger AN® 910 BPM	Chemtall (Hercules)	PAM/PAA Copolymer	High	4,200,000 (viscosity based)	n.a.	Anionic
Charge Neutralization						
Alcofix® 169	Ciba Specialty	Poly-DADMAC	Low	300,000 (mass based)	High	Cationic
Charge Patch						
Polymin® SKA (Modified PEI)	BASF	Modified PEI	Medium-high	2,000,000 (mass based)	High	Cationic

Coagulant: Poly DADMAC, Polyamines and PEI
Flocculant: High mass cationic polyacrylamide (Cat. PAM)

4.3 Device for evaluation of dewatering

Major apparatus: The Positive Pulse Jar (PPJ)

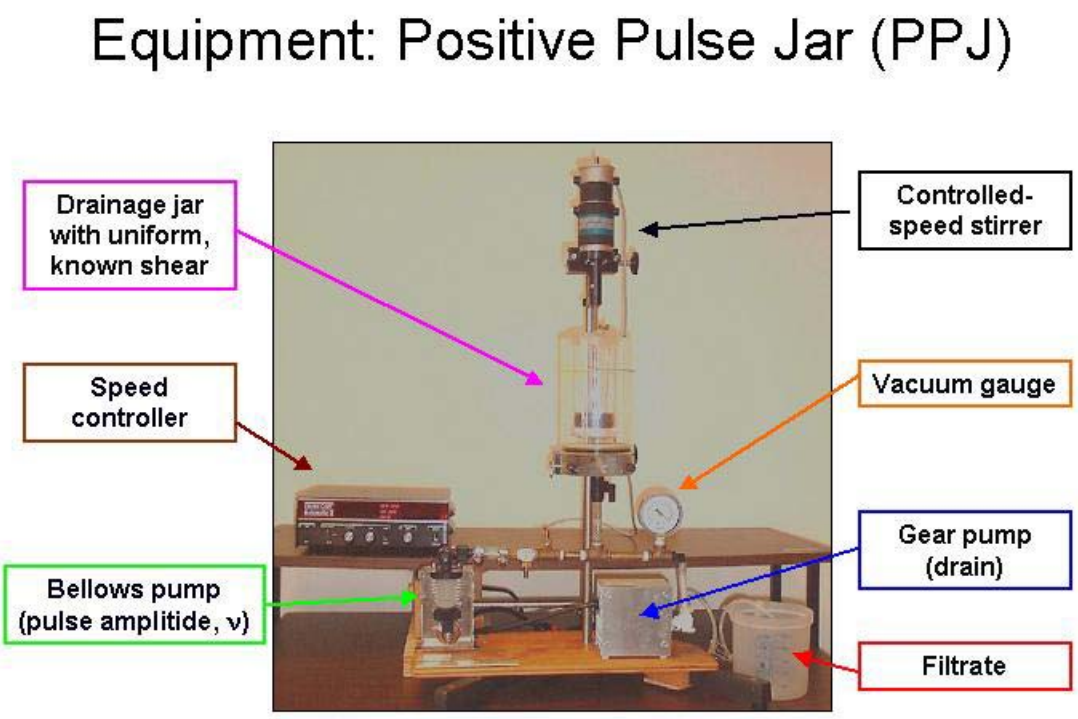

Figure 6 Positive Pulse Jar apparatus for evaluation effects of chemical additives on drainage resistance and final moisture under highly controlled conditions of mixing shear and pulsating flow to simulate the action of hydrofoils during formation of paper

The Positive Pulse Jar (PPJ), initiated by Dr. Martin A. Hubbe of NCSU, consists of the components shown in Figure 6. Plastic components of the device, and also the impeller stirrer, drive, and stand were taken from a Mark IV Dynamic Paper Chemistry Jar apparatus obtained from Paper Technology Laboratory, Inc. in Carmel, NY. An upper baffled chamber was equipped with a 200-mesh screen, a wire support, and a uniformly perforated plate located under the forming wire. A bellows pump created water pulsations of controlled frequency and amplitude, simulating the effect of hydrofoils and vacuum

elements on a commercial paper machine. Another special perforated plate (Figure 7) was put below the screen to make the flow created from the bellows pump pass more uniformly through the screen. It would tend to increase the resistance contribution of the apparatus (rather than the fiber mat), but it was necessary to distribute the pulse flow thoroughly. The differential pressure across the mat and forming fabric was induced by an external gear pump, which was connected to the filtrate container. The pressure/vacuum action can be observed on the gauge and the value can be used as an indication of resistance to dewatering at each stage in the process.

As an option, the PPJ also can be run so that the furnish is sheared uniformly either before or during a dewatering experiment. Above the wire, a rotating cylinder, the lower end of which is a truncated cone section was used inside a jar to generate a uniform shear rate on the wire of the device. After mat forming, the mass of the moist fiber pad can be determined by removing of a tared screen and weighing it.

Major component of Positive Pulse Jar

Inverted Cone

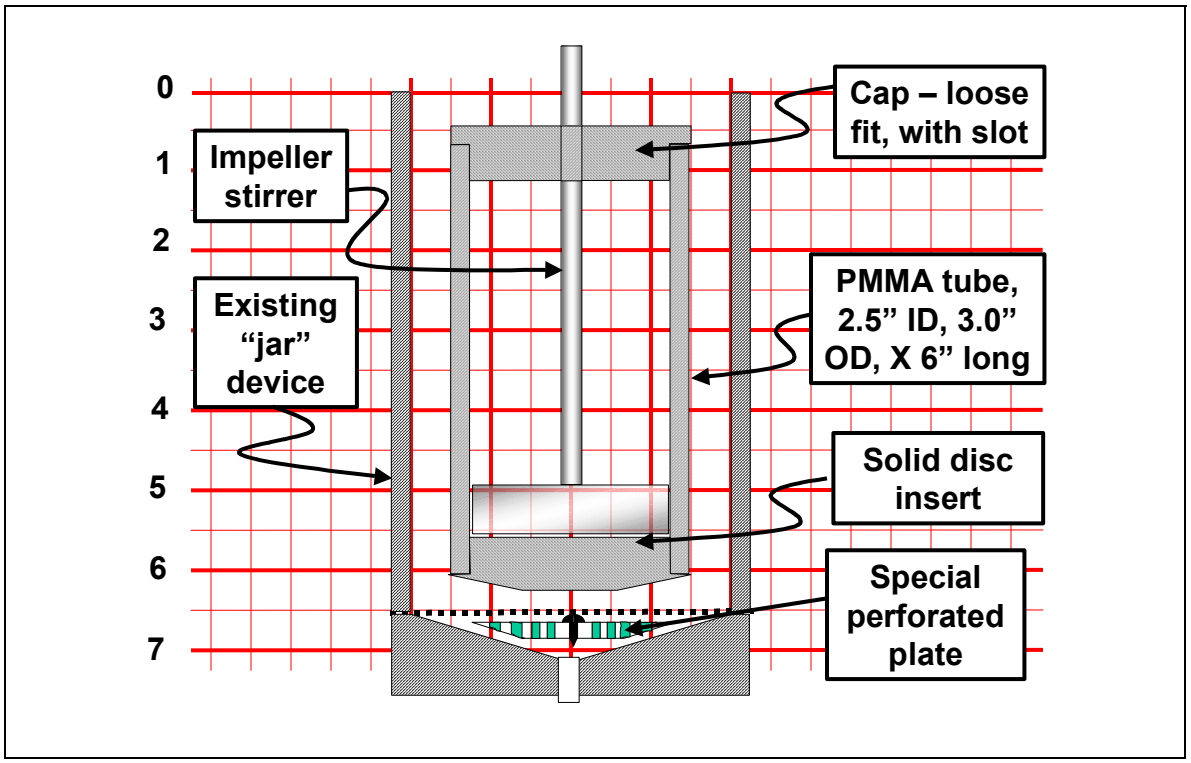

Figure 7 Detail of rotor that applies a nearly constant hydrodynamic shear field to papermaking furnish

The concept of uniform shear rotor was borrowed from the University of Maine (48). The difference between the uniform shear rotor in this experiment and the rotor from University of Maine is the shape of the rotor. The bottom parts of both rotors are almost the same shape. However, the body of the rotor in this experiment is a cylindrical shape. So, it has a side surface that the cone stirrer of University of Maine doesn't have. This new-designed rotor called the inverted cone was used in place of the original impeller of the jar to generate a known and uniformed shear rate in the PPJ. The cone has a 30^{o} angle at the bottom and has a 43.3 mm radius. The bottom part of the inverted cone is parallel to the mesh surface in order to reduce the flow forced by the cone rotor through the mesh. Under the mesh, a special perforated plate was placed to create a uniformed flow. The numbers in the figure refer to the scale in inches.

Bellows Pump

A set of three different sizes of bellows (0.5, 1.0 and 1.5 inch in diameter) from a Walchem Model SP80-30 pump were used to create pulsations of flow back and forth through the forming screen. The bellows was attached with a variable speed motor capable of 650 cycles per minute and a variable stroke (Bellows size selection was included in the Appendix C).

The pulsation action from sinusoidal compression of a bellows can be considered as a case of simple harmonic motion (SHM). The sinusoidal displacement of the bellow action as a function of time will basically follow the equation below.

$$Y = A \sin(2\pi f t) \tag{6}$$

Y = displacement in Y direction

A = amplitude

f = frequency

t = time

The pulse amplitude can be controlled by the size of bellows or by means of a stroke length adjustment on the outside rim of the cam body of the pump. The frequency of pulsation can also be adjusted by changing the speed of the connecting motor.

External Gear Pump

Figure 8 Schematic diagram of external gear pump (57)

An external gear pump normally uses gears that come in and out of mesh. As the teeth come out of mesh, liquid flows into the pump and is carried between the teeth and the casing to the discharge side of the pump. The teeth come back into mesh and the liquid is forced out the discharge port. External gear pumps rotate two identical gears against each other. Both gears are on a shaft with bearings on either side of the gears (57). In this experiment, an external gear pump was used to create a discharged flow rate of 26 ml/sec (specification).

Supporting apparatus: Turbidimeter, Fiber Quality Analyzer (FQA), and Sheet Splitter

Figure 9 DRT-15CD Turbidimeter

Turbidimeter: The turbidimeter used in the experiments was a DRT-15CD Turbidimeter from HF Scientific, Inc. The sample size of filtrate for each measurement was around 20–25 ml. Turbidity measures the effect of suspended solids on light passing through the sample. Particles in the liquid cause some of the light to be scattered, allowing it to be detected optically at 90 degrees relative to the incident beam. The higher the intensity of scattered light, the higher the turbidity value. Turbidity is commonly measured in Nephelometric Turbidity Units (NTU). In Nephelometric method, turbidity is measured by comparison of the light scattered by the sample and the light scattered by a standard reference solution. The human eye can perceive a turbidity of around 5 NTU or greater (58). Turbidity measurement is considered as a rough, quick, analytical tool, but it can give an approximate measure of the amount of solids in a suspension, especially if the results are supplemented by calibration tests.

Figure 10 Fiber Quality Analyzer (FQA)

Fiber Quality Analyzer (FQA): The Hi-Resolution Fiber Quality Analyzer, model LDA96, from Optest Equipment was used mainly to determine the percent fines content of pulp slurry samples. The device can also measure fiber length, fiber coarseness, curl

index and kink angle. Research showed that parameters measured by this model of the FQA are compatible with other standard equipment and methods (59). An additional experiment described in the Appendix D to this document showed that the FQA couldn't detect and measure filler particles. The standard definition of "fine particle" in this model of FQA is the particle that is smaller than 0.2 mm (200 micron). The percentage of fines from FQA is based on the total number of particles analyzed. A search of the literature revealed no publications showing the relation between the percent fines based on mass and the percent fines based on number.

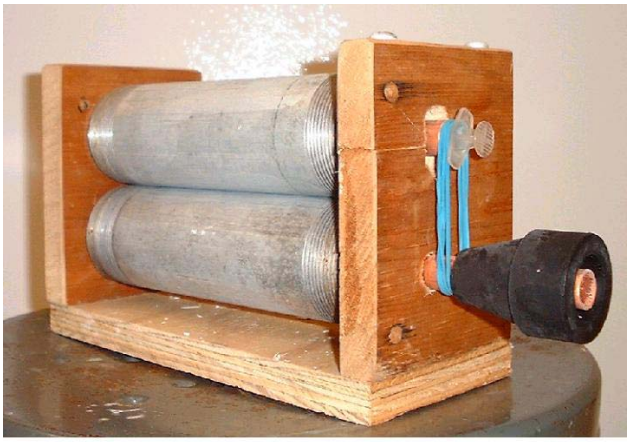

Figure 11 Prototype sheet splitter

Sheet Splitter: The Prototype Sheet Splitter was made by following the general principles of the Beloit sheet splitter (60). It is composed of two steel rolls that can be easily rotated. The sample is fed into the nip, where it contacts with the freezing surfaces of both steel rolls. Delamination happens when the user rotates the bottom roll at a constant speed. It was observed that the two split fractions usually are not equal in mass. The plane of delamination appears to depend on the distribution of mass, fines, and fillers

in the z-directional structure of paper (24). The samples after splitting were used to characterize z-directional distribution of material in the sheet. The percent fines in the sample were measured with the FQA device, and ash determinations were carried out in order to estimate the filler content. It is worth noting that the word " Total " used in this thesis means the combination of top layer and bottom layer in any parameters.

Surface charge of the system and Zeta Potential measurements:

Zeta potential was measured with the SKS Charge Analyzer. After adding a dilute colloidal suspension in a chamber, between two electrodes. The operator applies a potential across the electrodes. Looking through a microscope, the operator uses a stopwatch to time a speed of particle movement across a grid. It is first necessary to focus the microscope on the stationary plane of flow, about 14.7% into the chamber.

For streaming potential measurement, the Lab Zeta Data (Paper Chemistry Lab, Inc.) provides accurate data with the fiber pad technique described earlier.

Charge measurements were also done with a streaming current detector (Mütek PCDpH 03) and a Mütek PCD-T auto-titrator. The cationic standard titrant normally used in charge titration is Poly-DADMAC. The corresponding anionic polyelectrolyte titrant is potassium polyvinyl sulfate (PVSK).

5. EXPERIMENTAL PROCEDURES

A master batch of pulp slurry following the recipe in Table 1 was the major furnish of this project. The consistency of pulp slurry was diluted to 0.5% with deionized water.

The electrical conductivity was adjusted to 1000 μS/cm by addition of sodium sulfate. Three types of forming regimes as shown in Table 3 were the major independent variables in this experiment. All conditions were also examined at three levels of shear before PPJ dewatering. The low level of shear was 500 rpm of standard stirring. Medium shear was 1000 rpm of the same normal stirrer. A blender model 1154 from Dynamics Corporation of America was used to simulate the high level of shear, using the lowest speed of the blender. The stirring time for all conditions was 30 sec.

Table 3 Independent variables in experiments

Forming regime	**Simple filtration**	**Pulsation**	**Shear exposure**
Pre-parameters (Before PPJ drainage)	Low-shear level, Medium-shear level, High-shear level	Low-shear level, Medium-shear level, High-shear level	Low-shear level, Medium-shear level, High-shear level
Post-parameters (During PPJ drainage)	none	Selected amplitudes and frequencies	Type of Stirrer: Inverted cone and Standard Stirrer @ 500 rpm

It should be pointed out that the simple filtration mechanism in this experiment was not a simple gravity dewatering. It was controlled at a constant rate of dewatering imposed by the external gear pump.

Basic procedures of PPJ

With reference to Figure 6, the dewatering tests were carried out using the following procedures:

1. Completely fill the lower compartment of the apparatus with deionized water until no air bubbles remain.
2. Pour the prepared fiber slurry (500 ml) into the upper part of the apparatus, above the screen.
3. Initiate stirring at a controlled rate and time.
4. Add chemicals at the desired dosages, sequence, and times.
5. Discontinue agitation.
6. Initiate pulsation (bellow pump shown at left of figure) and dewatering (gear pump shown at right of figure). Also record pressure (vacuum) output continuously.
7. Discontinue pulsation after the water level reaches the dry line.
8. Stop the gear pump 10 seconds after appearance of the dry line.
9. Remove the upper portion of the apparatus (deckle), exposing the screen.
10. Remove the wet mat together with the tared screen and determine the mass immediately.
11. Analyze the filtrate quantitatively or qualitatively, such as filtrate volume, solids content of the filtrate, turbidity of filtrate, *etc*.
12. The wet sheet can be couched onto a blotter paper and dried to determine the solids content or moisture content of the wet mat (TAPPI Method T550 (61)).

13. Further auxiliary analysis can be done such as unevenness of formation, sheet splitting and filler content (TAPPI Method T 211(62)).

Note: Steps 3 to 5 can be done in other containers or stirrers with specific conditions before adding the slurry into the jar. We can also use the PPJ in a DDJ mode (as in the classic Britt Jar test procedure) if we replace the inverted cone with the standard stirrer.

Fines content determination (63)

FQA Analysis was used to determine the fines content of the sample. The total count of particles in a test was set at 2000 particles. The events per second (EPS) during analysis was automatically set by the equipment at around 40. This is the average number of fibers and fines which are being analyzed by the FQA per second. The sample was diluted until its consistency didn't exceed the EPS value during measurement.

Ash content determination (62)

Ash content determination was done following the Tappi Method T211, with the following modifications. The oven-dried sample was weighed and put in the known-mass crucible cup. It was put in a furnace at about 100 ^{o}C. The temperature of the furnace was raised up to 525 ^{o}C gradually. To make a complete combustion and avoid black spots or black particles from incomplete ashing, the sample was kept in the furnace over night. When the sample was completely combusted, the crucible with ashed sample was removed and placed in a desiccator for 30 min. Then the mass of the crucible cup with sample was determined and used to calculate the ash content. Other researchers suggested

to perform the ashing at 400 ^{o}C overnight (16 hrs) to reduce the decomposition of filler due to high temperature and long-time ashing (64).

6. RESULTS AND DISCUSSION

Experiments before PPJ dewatering

6.1 Effect of different pre-shear levels on fines content

In this experiment the pulp sample was prepared following the recipe in Table 1. It was also prepared in different batches to check the reproducibility of experimentation. A volume of 500 ml of sample was taken per batch and exposed to the different levels of shear before dewatering in the PPJ. Descriptions of the procedure used for creating different shear levels were already given in the experiment and procedure section.

Table 4 1st experiment: Dec 21, 02

Sample	FQA, Fines (%)			Average	SD
No Shear	77.37	76.60	78.20	77.39	0.80
Low Shear	77.07	76.10	77.67	76.95	0.79
Med Shear	76.57	75.40	76.00	75.99	0.59
High Shear	77.53	77.37	76.77	77.22	0.40
				76.89	

Table 5 2nd experiment: Jan 5, 03 (Batch 1)

Sample	FQA, Fines (%)			Average	SD
No Shear	73.73	74.33	75.87	74.64	1.10
Low Shear	76.73	73.83	77.27	75.94	1.85
Med Shear	74.17	76.17	75.47	75.27	1.01
High Shear	75.43	74.73	75.43	75.20	0.40
				75.26	

Table 6 3rd experiment: Jan 5, 03 (Batch 2)

Sample	FQA, Fine (%)			Average	SD
No Shear	74.50	75.40	75.83	75.24	0.68
Low Shear	75.60	73.93	74.97	74.83	0.84
Med Shear	76.07	74.97	75.47	75.50	0.55
High Shear	75.67	74.37	73.43	74.49	1.12
				75.02	

Tables 4 to 6 show the effect of shear on the stock fines content. The goal of this experiment was to determine what happens with the furnish slurry under shear exposure. This was done because interpretation of results in the next step would be more difficult if the shear force changes the characteristics, for example, fines content, of furnish. To make sure that the experiments were good in statistical aspects, the experiments were separately prepared in three batches in different periods. Then, these slurries were exposed to the shear at different levels. The furnish recipe and the conditions of shear level can be found in the experimental part. Fines content was determined by FQA.

When different levels of shear were applied to the pulp slurry before sheet forming, it is reasonable to assume that there was no change of fines content in the case of replicate tests within the same batch of pulp. However, the average value of the fines content in one batch differed from the fines content in other batches that were prepared at other times. This difference may come from variations in furnish preparation. Such variations in fines content from batch to batch may help to explain why some of the indicated ranges of standard deviation appear quite wide, although data all obtained from single furnish batches showed less variation in replicate tests.

6.2 Effect of forming regimes on pressure/vacuum responses

To understand the behavior of the drainage process in the PPJ, the pressure/vacuum value was observed as a function of time during the application of different forming regimes. The pressure/vacuum value could be observed from the pressure/vacuum gauge. The movements of the gauge's indicator during drainage were observed and sketched as shown in the figure below.

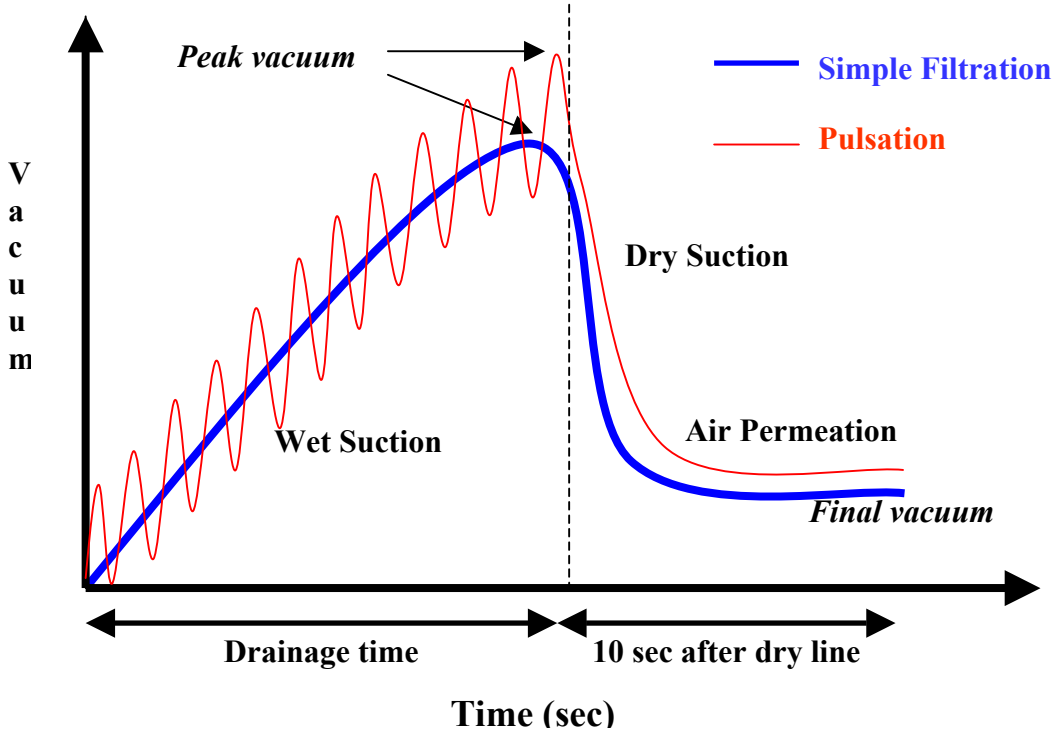

Figure 12 Schematic of observed vacuum curve during drainage in PPJ

Figure 12 shows the observation of pressure/vacuum values of the dewatering processes in the PPJ. In the system, changes in the pressure/vacuum responses to the furnish drainage under the influence of a constant flow rate of the external gear pump

(volume/time) were measured as a function of time. In simple filtration, the value of vacuum reading gradually rose until it reached the peak value (peak vacuum) because the resistance of water flow increased. Then, the sheet was compressed and the dry line appeared. This peak vacuum was dependent on the type of forming regime. A few seconds later, the vacuum dropped as air was sucked through the channels in the sheet. We may use the time from the starting of drainage to the dry line appearance as a measure of drainage time. After the dry line, vacuum action was further continued 10 sec and the gauge showed a constant value of vacuum. In case of pulsation, the vacuum-gauge indicator went up and down during the dewatering process. The average value of vacuum reading was almost the same value as those in the simple filtration at the same time. The peak vacuum of the pulsation drainage was higher than that in simple filtration, possibly due to the fluctuation of pulsation effects. The pulsation pump was manually stopped at the beginning of the dry line, but the suction from the gear pump was further continued 10 sec. In the case of shear application during dewatering (not shown in Figure), the responses of vacuum gauge of inverted-cone rotor and impeller varied in an unpredictable manner. Both types of stirrer tended to create a suction force above the wire. So, the peak vacuums from both stirrers were higher than those in simple filtration. The suction effect from both stirrers created activity above the wire and resulted in a high amount of solid content in the filtrate. This was confirmed by the turbidity measurements as shown in Table 7.

Table 7 Vacuum responses and turbidities of different forming regimes

Description	Peak Vacuum (kPa)	Final Vacuum (kPa)	Filtrate Turbidity (NTU)
Simple Filtration	41	20	169
2 Hz, Full Stoke	52	20	284
Inverted Cone	69	not constant	351
Impeller	58	23	168

Compared with other previous work, the shape of the drainage curve in Figure 12 was quite similar to a typical reported curve created on the DDA (10) but it was different from a typical result plotted in the G/W drainage analysis system (9). However, other parameters can be used as the indicators instead of vacuum responses. The drainage time, drainage rate, and accumulated filtrate volume were some examples of indicators used in previous work (11).

6.3 Effect of frequency and stroke of bellows pump on amplitude

Laboratory evaluations of pulsation effects could be done by several techniques. Pressure pulses of air were a convenient way to create pulsation by opening and closing air valves (6). The pulsation created by the interaction of cogs and moving belt can be found in MBDT. However, such devices were mechanically complex and the amplitudes of the pulses were not easily controlled. In addition, some vacuum-driven systems also responded too slowly to achieve the range of frequencies of pulsation associated with a commercial paper machine. However, the PPJ device is able to control both frequency and amplitude of pulsations. Due to the insensitivity of a pressure/vacuum gauge to the rapid change of frequency, an additional experiment was set to investigate the effect of

the output pulses of the bellows pump on the mat. The jar was removed and replaced with a plastic hose (approximately 0.25 inch ID). A scale was connected beside the hose to determine the displacement of the water movement in vertical direction. A few drops of blue dye were added to the water to create a clear observation. The measured parameter was the difference of distance between the highest water level and the lowest one. The amplitude or displacement was considered as half of the water level difference.

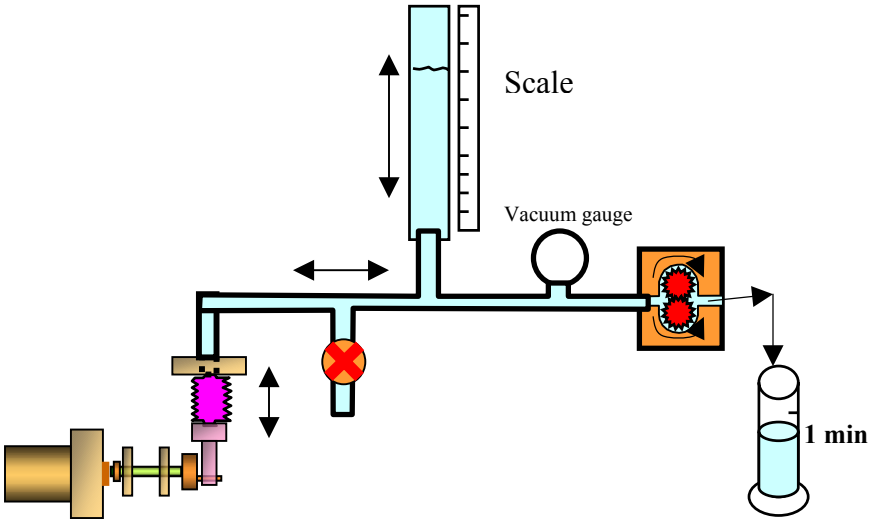

Figure13 Equipment set-up for calibrating pulsation effect

Figure 13 shows the height differences of water levels from pulsation effects at different frequencies and stroke lengths. The average values in height difference of each condition were plotted in Figure 14. Regardless of the friction of the plastic hose and the moment of inertia of the water motion, it is likely that the higher stroke length gave higher amplitude. It was also observed that the height differences or pulse amplitudes decreased apparently when the frequency of the bellows pump increased. This may be explained

based on the fact that the friction in the system had reduced the intensity of the pulsation from the bellows movements. So, the output pulsation would be less than the input pulsation. At very high frequency level, the pulsation effect was very small, and the drainage seemed to perform like simple filtration drainage.

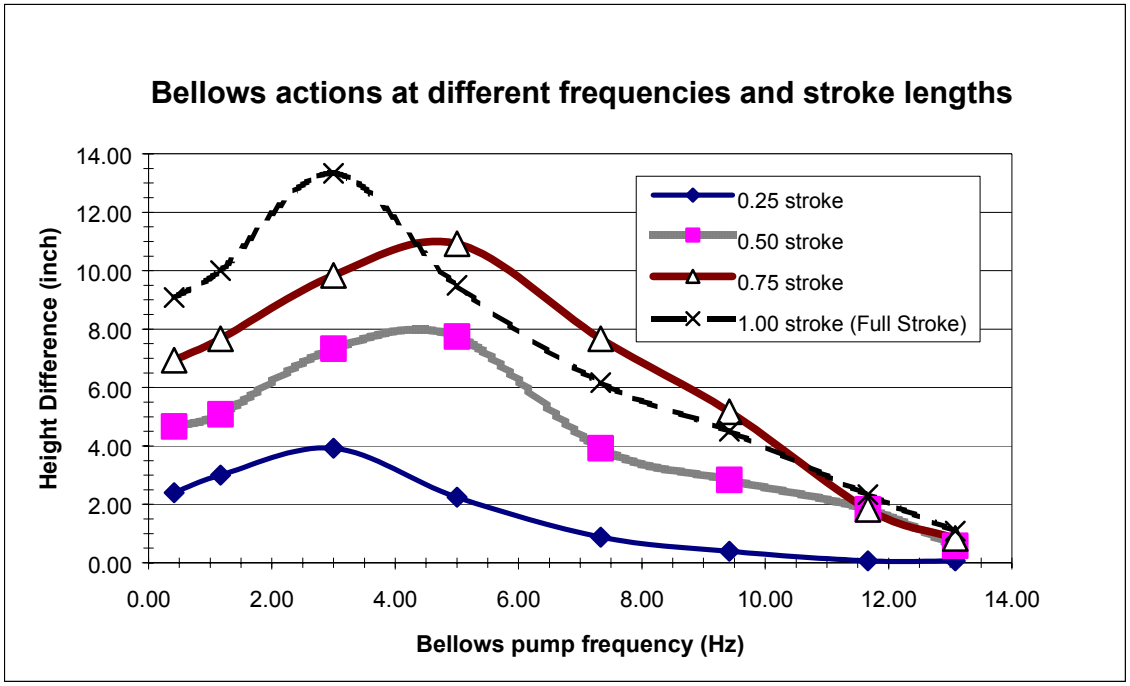

Figure 14 Bellows actions at different frequencies and stroke lengths

6.4 Effect of frequency and stroke length of bellows pump on flow rate of external gear pump

Besides the effect of frequency and stroke length on pulsation, another effect from the external gear pump played a role in the pulsation behavior. The purpose of the external gear pump is to speed up the dewatering process by sucking the filtrate out. In the experiment, the fiber slurry contained a lot of fines and filler particles. These small

particles are expected to retard the flow of drainage. To understand the drainage characteristics of the PPJ, study of external gear pump behaviors should be done. The experiment was set up in the same manner as in Figure 13. The one-minute filtrate was collected at different stroke length and frequency. The filtrate volume was determined and calculated as flow rate.

Table 8 Effect of frequencies and stroke lengths on gear pump performance

Speed No.	**Flow rate (ml/sec)**			
	0.25 stroke	**0.50 stroke**	**0.75 stroke**	**1.00 stroke**
0	26.53	26.47	26.75	26.01
2	26.71	26.41	25.89	25.85
4	26.36	26.06	24.67	26.85
6	26.25	26.71	26.15	27.03
8	26.27	26.78	26.62	26.27
10	26.53	26.77	27.53	26.34
			Average	**26.41**

Table 8 shows the effect of stroke length and motor speed no. (frequency) on the flow rate of the gear pump. Based on these results it is reasonable to expect that there was no significant change in average flow rate due to the gear pump action during dewatering tests due to differences in stroke length and frequency of the bellows pump. This would imply that the flow rate of the gear pump was not affected by the frequency and stroke length change. The observed flow rates also were consistent with the flow rate specification of the gear pump (26 ml/sec). This result was helpful in calculating the magnitude of a pulsation effect in the PPJ. Since the pulsation movement was based on simple harmonic motion, the net vertical pulsation velocity at the plane of the forming fabric in the PPJ device obeyed the equation below. Details pertaining to Equation (7) can be found in Appendix E.

$$V = 0.0439\, X_{SL}\, (2\pi f)[\mathrm{Cos}(2\pi f t)] - 0.331 \qquad (7)$$

V = Velocity, cm/sec

X_{SL} = Fraction of full stroke length (0 to 1)

f = Frequency, Hz

t = Time, sec

From equation 7 it is possible to calculate the velocity of pulsation from bellows actions under different conditions of fractional stroke length (amplitude) and frequency. Calculated maximum and minimum velocities for different combinations of frequency and stroke length of bellows pumping are shown in Table 9.

Table 9 The maximum and minimum velocity of pulsation in PPJ at different frequency and amplitude of bellows (calculated from equation 7)

Stroke length ratio	**Frequency (Hz)**	**Flow velocity (cm/sec)**	
		Maximum	**Minimum**
0.125	**16 (max.)**	**0.221**	**-0.883**
0.25	**8**	**0.221**	**-0.883**
0.5	8	0.773	-1.435
0.5	**4**	**0.221**	**-0.883**
1.00 (Full stroke)	8	1.877	-2.539
1.00 (Full stroke)	**2**	**0.221**	**-0.883**

It is worth noting that for a constant stroke length*frequency product, the flow velocity is also constant (see data in bold number in Table 9). The flows that occurred on the mat of the PPJ were both upward and downward, which can be observed from the signs (minus

sign means the flow in the suction direction and plus sign means the flow which occurred opposite to the suction direction).

6.5 Effect of pulsation on in-plane fines distribution

It has been believed that stirring affects the orientation of the fibrous material during mat forming. In the experiment, the effect of stirring on mat formation was investigated. The sample prepared following the recipe in Table 1 was put into the PPJ. The default value of the impeller speed in the PPJ tests was set at 30-sec stirring before the dewatering process started. In the pulsation condition, the bellows pump was started immediately after the stirring process finished. The filtrate was collected from each condition and the fines content was measured with the FQA. The results are shown in Table 10 below.

Table 10 Difference between simple filtration and pulsation on in-plane fines distribution

Description	Shear in PPJ	Position	Side	FQA, %Fines				
				1st	2nd	3rd	Average	SD
Simple Filtration	Low	Center	Top	71.47	72.47	71.70	71.88	0.52
			Bottom	74.17	72.20	73.37	73.25	0.99
		Edge	Top	74.23	74.93	74.53	74.56	0.35
			Bottom	75.63	77.30	76.13	76.35	0.86
8 Hz 0.5 stoke	Low	Center	Top	72.17	73.70	73.47	73.11	0.83
			Bottom	70.50	71.50	72.33	71.44	0.92
		Edge	Top	73.40	74.30	72.20	73.30	1.05
			Bottom	71.40	72.40	72.03	71.94	0.51

Results in Table 10 show that the stirring process affected mainly the results of tests involving the simple filtration mode. The fines content at the edge position was higher

than that at the center position in both top and bottom parts of the fiber mat. However, the fines content of the top part of the mat was less than that in the bottom part, both near the center and near the edge of the mat. In the pulsation mode, the mat forming was more uniform in in-plane fines distribution. The fines content at the center and the fines content at the edge were almost the same percentage. In the z-direction, the fines content in the top part of the mat was higher than the fines content in the bottom part, due to the effect of pulsation.

6.6 Effect of pulsation on z-directional fines and filler distribution

In industrial-scale papermaking, the forming process has the largest effect on fines and fillers distributions (15). The drainage flow mainly carries these small particles with it in one direction. This movement leads to an uneven distribution of fillers and fines. However, the aggregation of fines and filler is also undesirable because this results in decreased light scattering (13). In previous work, Van de Ven concluded that the rate of fines and filler deposition on a fiber attains its maximum, depending on the balance between colloidal and hydrodynamic forces (50). The shear effect in the flow tends to break the fiber-fiber flocs more easily than the bonds of fiber-fines flocs or fiber-filler bonds. In the experiment, the master batch of stock was prepared with the ratio of material specified in Table 1. The pre-shear levels were not applied in this experiment. Three replicates were done in each condition to ensure the good repeatability of the study. The mats formed under different conditions were removed and split with the sheet splitter. Each part of the sample was used to determine the fines content and filler content

with FQA and Ash determination. The results of fines distribution are presented in Table 11. The filler distribution in z direction can be found in Table 12.

Following the results in Table 11 and 12 below, it is likely that both fines and filler content of the top part were greater than those of the bottom part in both drainage regimes. A possible explanation is that these phenomena may be due to the suction of the external gear pump. Both filler and fines located close to the wire were easily removed by washing action. The pulsation tended to create more difference in the top and bottom part of filler and fines content than the simple filtration did. This result was consistent with other results such as turbidity, total ash content, and ash retention.

Table 11 Effect of pulsation on filtrate turbidity and fines distribution

Description	Side	% of Layer (mat)	Filtrate Turbidity (NTU)	FQA, %Fines					Avg Top	Avg Bot
				1st	2nd	3rd	Avg	SD		
Simple	Top	68.36	105	83.38	80.67	79.63	81.23	1.94	80.16	77.11
Filtration	Bot	31.64		75.97	78.03	76.13	76.71	1.15		
(3 replicates)	Top	71.49	101	78.77	79.17	78.43	78.79	0.37		
	Bot	28.51		74.77	74.87	76.47	75.37	0.95		
	Top	74.67	104	80.43	81.13	79.80	80.45	0.67		
	Bot	25.33		78.63	80.20	78.95	79.26	0.83		
Average			103							
8 Hz	Top	68.12	245	83.60	84.87	83.63	84.03	0.72	80.54	76.05
Full Stoke	Bot	31.88		74.90	76.49	79.17	76.85	2.16		
(Pulsation)	Top	63.15	230	82.20	80.57	79.43	80.73	1.39		
(3 replicates)	Bot	36.85		78.13	77.90	77.20	77.74	0.48		
	Top	78.27	238	78.17	77.00	75.43	76.87	1.37		
	Bot	21.73		74.06	70.53	n.a.	72.30	2.50		
Average			238							

Table 12 Effect of pulsation on filler distribution

Description	Side	%Layer (ash)	Ash Content (%)		Ash Content (%)		Total Ash	%Ash Retention
			Top (70% of layer)	Bottom (30% of layer)	Average (top)	Average (bottom)	(%)	(total)
Simple	Top	64.79	23.39	26.70	23.78	22.62	25.05	90.13
Filtration	Bot	35.21						
(3 replicates)	Top	75.95	23.19	19.45			21.32	77.07
	Bot	24.05						
	Top	77.78	24.76	21.70			23.23	84.00
	Bot	22.22						
Average							23.20	83.73
8 Hz	Top	80.36	25.83	16.33	23.17	14.76	21.08	74.67
Full Stoke	Bot	19.64						
(Pulsation)	Top	70.74	18.28	14.06			16.17	57.87
(3 replicates)	Bot	29.26						
	Top	90.72	25.39	13.89			19.64	70.40
	Bot	9.28						
Average							18.96	67.64

6.7 Effect of stirrer and inverted cone on turbidity

It is possible to estimate the levels of hydrodynamic shear in different unit operations on a typical paper machine (14). To meet this purpose, the Britt jar has been used as a popular lab method for the last few decades. In Britt jar applications, evaluations of the retention aids performance can be done by use of an adjustable speed-controlled impeller to represent the net effects of such operations. The jar test is "calibrated" by adjusting the stirring speed so that the retention of fine materials observed in the lab matches the retention efficiency observed on the paper machine. The typical speed of impeller in Britt jar retention experiment was set at 500 rpm. This can be approximately estimated as a

level of shear of rectifier roll in a headbox (65). A 1000 rpm stirring of Britt jar impeller was roughly considered as a condition of shear created by the hydrofoil (65).

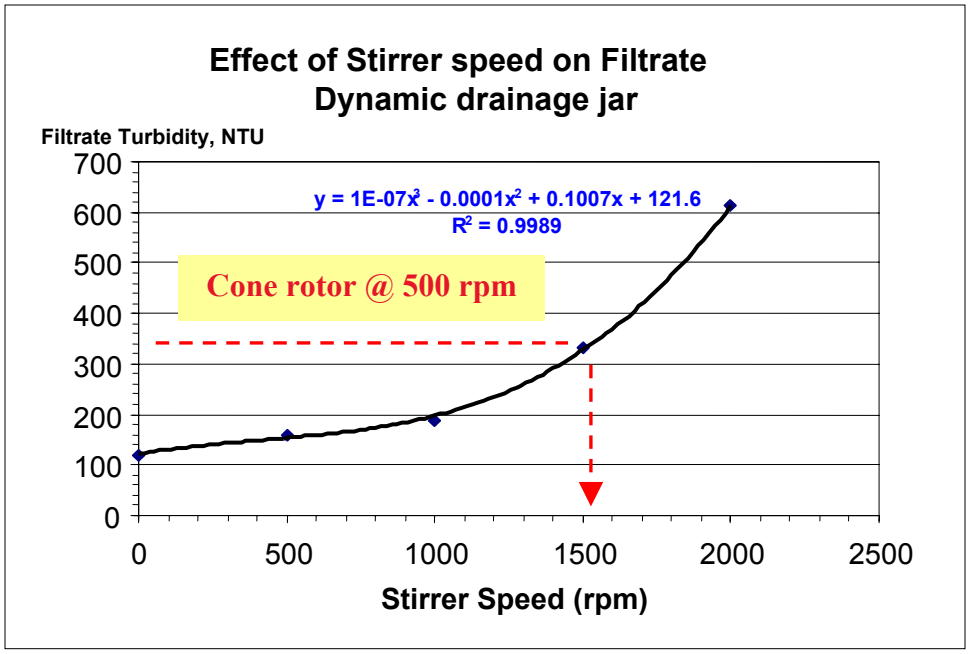

Figure 15 Calibration of the inverted cone speed with the typical stirrer

Figure 15 shows results of calibration of the inverted cone in the Britt Jar mode. The turbidity was used as a quick indicator for retention evaluation. The inverted cone rotor was set at 500 rpm constantly due to splashing phenomena that made higher speeds impractical. Results showed that use of the inverted cone at 500 rpm gave the same level of turbidity in the filtrate as use of the typical stirrer at 1500 rpm. This result implied that the inverted cone created more shear effects than those created from the typical stirrer at the same speed. This would be confirmed by the responses of pressure/vacuum value and turbidity measurements in topic 6.2.

Experiments in PPJ with retention aids

6.8 Chemicals dosage in each retention aid system

In this part of the study, many chemicals were used in different kinds of retention aid system. It is believed that the dosage of cPAM in the single-polymer bridging system should not be more than the neutralized dosage to avoid the possibility that a steric stabilization mechanism might become important. However, the Poly-DADMAC used in the dual-polymer bridging system may be used at the excess amount of the neutralized amount to cover the surfaces more fully which cationic material that can serve as adsorption sites for aPAM. In the charge neutralization and charge patch systems, the agglomeration effect mainly relied on charge mechanisms. So, it would be better idea to evaluate any parameter at the neutral point condition. Table 13 shows the amounts of chemicals used in the experiments.

Table 13 Neutralized dosages of each chemical in thesis

Mechanisms	Neutralized Dosage (% on dry mass)	Dosage (% on dry mass)
Bridging ***Single Polymer*** Percol® 455 (cPAM)	**0.20%** **(Zeta = 0)**	**0.10%**
Dual Polymer Alcofix® 169 (Poly-DADMAC)	**0.10%** **(Zeta = 0)**	**0.20%**
Floerger AN® 910 BPM (aPAM)	**0.05%**	**0.05%**
Charge neutralization Alcofix® 169 (Poly-DADMAC)	**0.10%** **(Zeta = 0)**	**0.10%**
Charge Patch Polymin® SKA (Modified PEI)	**1.10%** **(Maximum drainage & Zeta = 0)**	**1.10%**

Coagulant: Poly DADMAC, Polyamines and PEI
Flocculant: High mass cationic polyacrylamide (Cat. PAM)

As we knew that the stock slurry in this experiment contained a lot of fines and fillers, we expected that the surface charge of this pulp slurry should be high and that it would result in a high dosage of these chemicals. Only the anionic PAM was used at the usual dosage corresponding to industrial practice. It is likely that the amount of modified PEI was more than CPAM and Poly-DADMAC to balance the charge of the system. This result may be explained that the modified PEI had some reduction in cationicity due to the high pH condition (pH = 9.1) (50). The dosage of CPAM was also more than the Poly DADMAC because of the low-charge character of CPAM itself. In the experiment, charge properties were mainly detected in the zeta potential mode with the SKS charge

analyzer (CPAM, Poly DADMAC) due to the ease of getting results. The neutralized dosage in some conditions was compatible with the neutralized dosage from the streaming current detector (Mütek PCDpH 03). Only the modified PEI was measured in the fiber pad streaming potential device because this device also provided the drainage information at the same time.

6.9 How different forming regimes affect retention and drainage aid programs

In this section, experiments were carried out to study the effects of different forming regimes on the performances of different retention aid systems. The results are shown relative to many types of dependent variables such as filtrate turbidity, total fines content, total retention, and ash retention. The results corresponding to each retention aid system will be presented after a description of results from the control experiments.

Control Set (No retention aids)

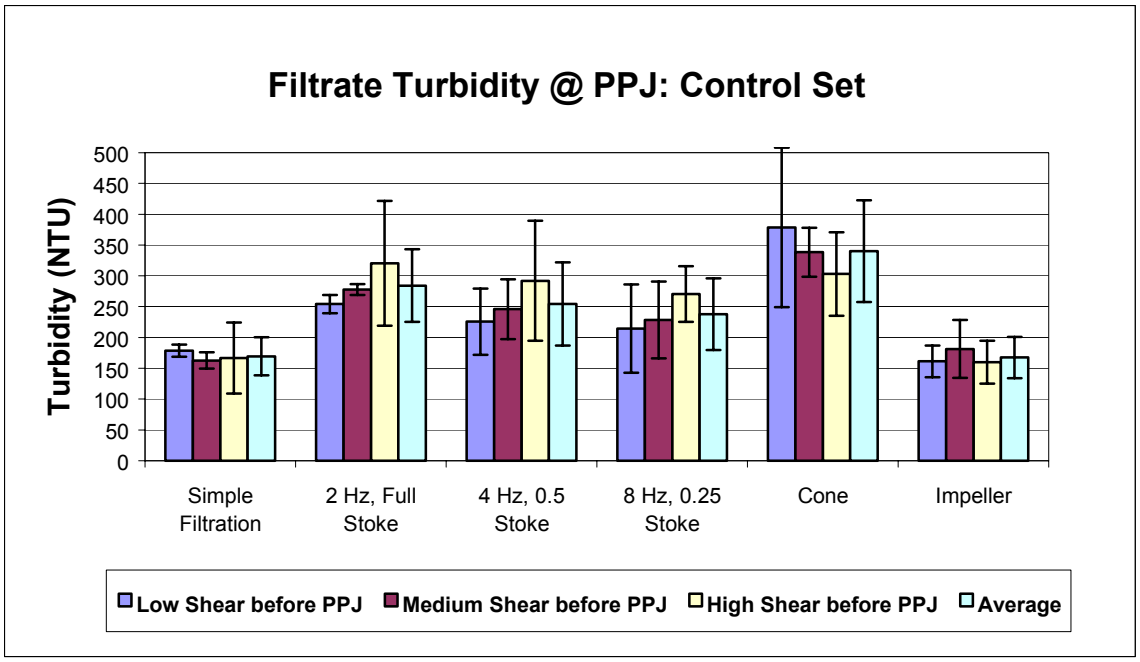

Figure 16 Filtrate turbidity results of different forming regimes (control set)

Figure 16 presents filtrate turbidity data of the control set experiments. The error bars in the figure show the standard deviation of measurement within each set of experiments. The filtrate turbidities from the cone stirrer had the highest value compared to those from other forming regimes. Following the data from section 6.7, the cone stirring at 500 rpm created the same turbidity value as the impeller did at 1500 rpm. One logical conclusion that could be drawn from this observation is that those two conditions of stirring produce approximately equal values of average shear stress. This may be the reason for an increase of turbidity in cone stirring. In the pulsation mode, the highest frequency and the lowest stroke length showed the lowest value of turbidity. These data are consistent with the results in section 6.3, which showed that a higher frequency or a lower stroke length resulted in less interruption of the mat. It was observed that pulsation at very high frequency and low stroke length almost had no effect on mat forming, leading to results

that were similar to the case of simple filtration. Finally, it seemed that the different levels of shear didn't create significant changes in the turbidity. The results showed wide ranges of standard deviation in almost all of the experiment sets. This may be explained as due to the fact that the pre-shear effect didn't change the properties of slurry (section 6.1) and each of the forming methods performed the same action on the fibers and fines within each group of pre-sheared suspensions.

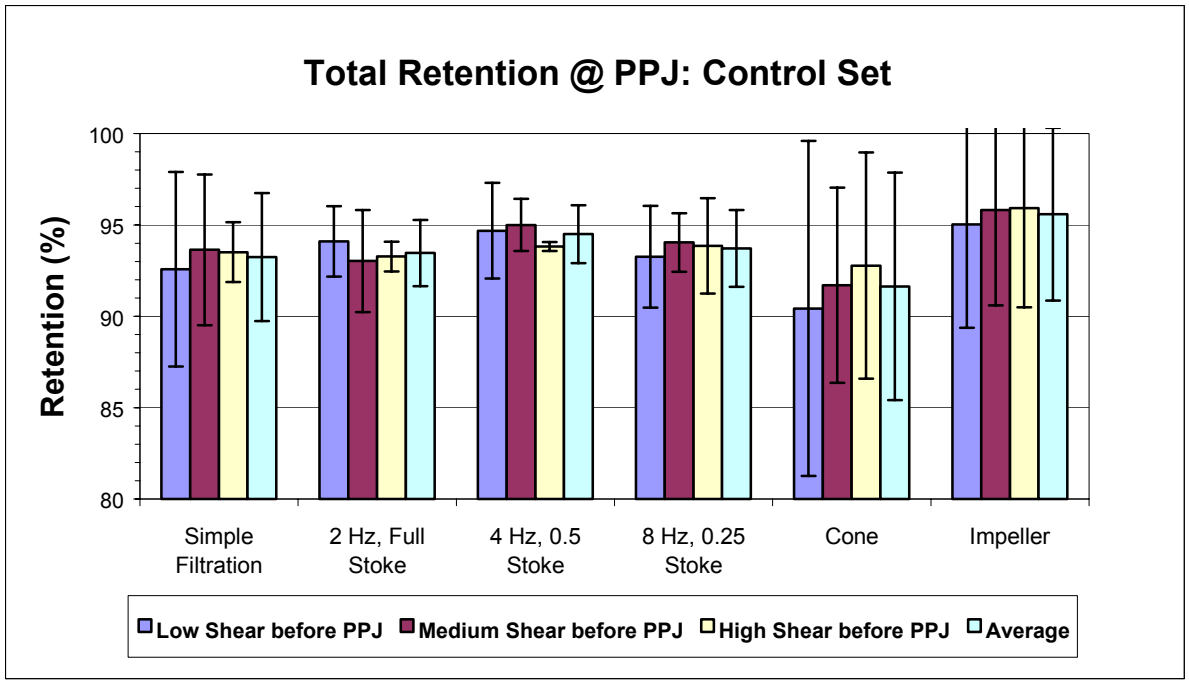

Figure 17 Total retention of different forming regimes (control set)

Figure 17 shows the retention efficiency for each of the forming regimes. The method of first pass retention in this experiment was different from the usual method. In the typical method, the consistency of the initial slurry and filtrate are determined, and these values are used to calculate first pass retention. In this experiment first the mass of the wet mat was measured. The results were used with the dry mass of the initial slurry to calculate the first pass retention. The results showed that the random error in these results was

quite high relative to the mean values. This maybe came from the errors from retention determination technique. The critical step is the dry mass determination. Because a set of samples were done and weighed in the same time, a sample could easily absorb the moisture from the surroundings after several openings of the desiccators. However, the results were sufficiently precise to show that total retention resulting from cone stirring was lower compared to results of other forming regimes. This is consistent with the results from turbidity tests and the results of experiment in section 6.7.

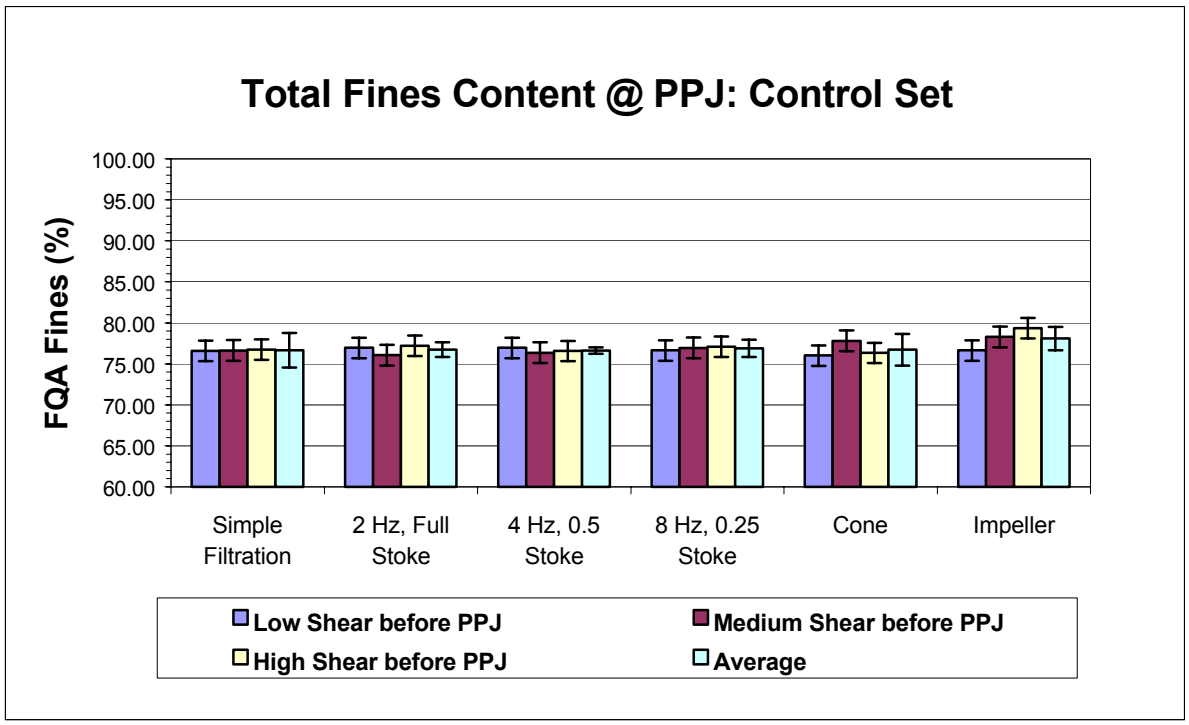

Figure 18 Total fines content resulting from different forming regimes (control set)

Figure 18 introduces the results of total fines content, as measured with the FQA device. Fines were measured from the sample retained on the wire. The results showed no significant differences between experimental conditions. This observation may be explained based on the range of values used for FQA measurements in determination of

fines content. By definition of FQA fines, a particle which is smaller than 200 microns will be considered as a FQA fine. However, the mesh hole opening in the forming fabric employed was 76 microns in diameter (200 mesh). That means the FQA measurements included the effect of particles ranging between 76 to 200 microns in their calculations. These particles, which are easily trapped on the mat, would reduce the difference of fines content in each condition. By contrast, the turbidity test, which is known to be sensitive to the presence of smaller particles in the filtrate (less than 76 microns), was found to be more reliable than the FQA.

It is worth noting that the control set didn't have any effect from retention aids. In that case it makes sense that researchers may use FQA for the purpose of fines determination. However, in the case of retention aids, the fines and fillers are expected to at least partly attach to the fibers surfaces. Researchers should be concerned about the level of shear force needed to separate these particles before using the FQA. Moreover, some reversible phenomena can be found in some retention aids programs; these effects should be concerned for any test depending on optical principles, such as the FQA and turbidity tests.

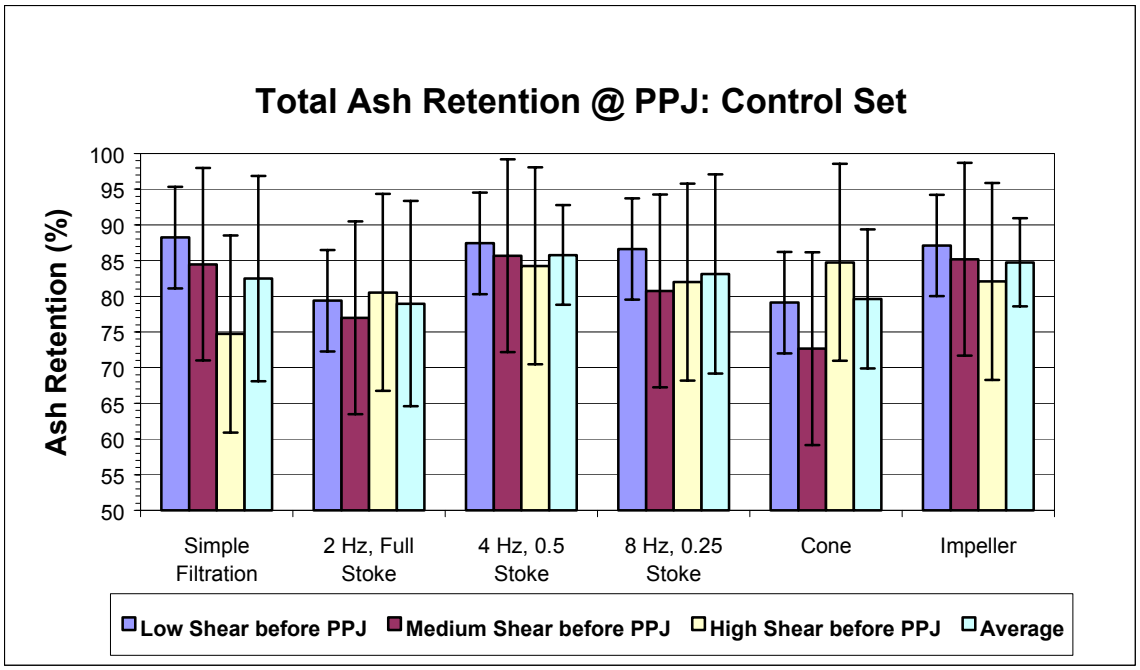

Figure 19 Total ash retention of different forming regimes (control set)

Figure 19 shows the effects of different forming regimes on total ash retention. The overall trend shown by the plotted bars seemed to be similar to those shown for total retention in Figure 17. This phenomenon may imply some correlation between ash retention and total retention. It is reasonable to suppose that the total mass of material on the mat might be mainly affected by the loss of filler into the filtrate. The standard deviations within each experimental set were very high in value. This made the results more difficult to interpret. The possible error may come from the human error in procedure of ash determination. However, the cone stirrer showed the lowest value in ash retention, excluding the set with 2 Hz frequency and & full stroke amplitude.

It should be pointed out that compared with the fines content in Figure 18, the ash retention showed some trends with more highly contrasting results. Such results can be

rationalized by the fact that the fillers are mostly smaller than the fines in size. In principle it would be easier for filler particles to pass through the opening of the mesh. This loss of filler could be more easily detected than the loss of fines from the mat.

Single Polymer Bridging

In the single polymer bridging system, the pulp slurries following the recipes in Table 1 were mixed with the cPAM at a dosage of 0.10% on dry mass (200 rpm, 30 sec). Different shear levels were applied to the pulp after mixing but before PPJ drainage. Different types of forming regimes on the PPJ were applied during formation of the mat in the case of those pulp slurries.

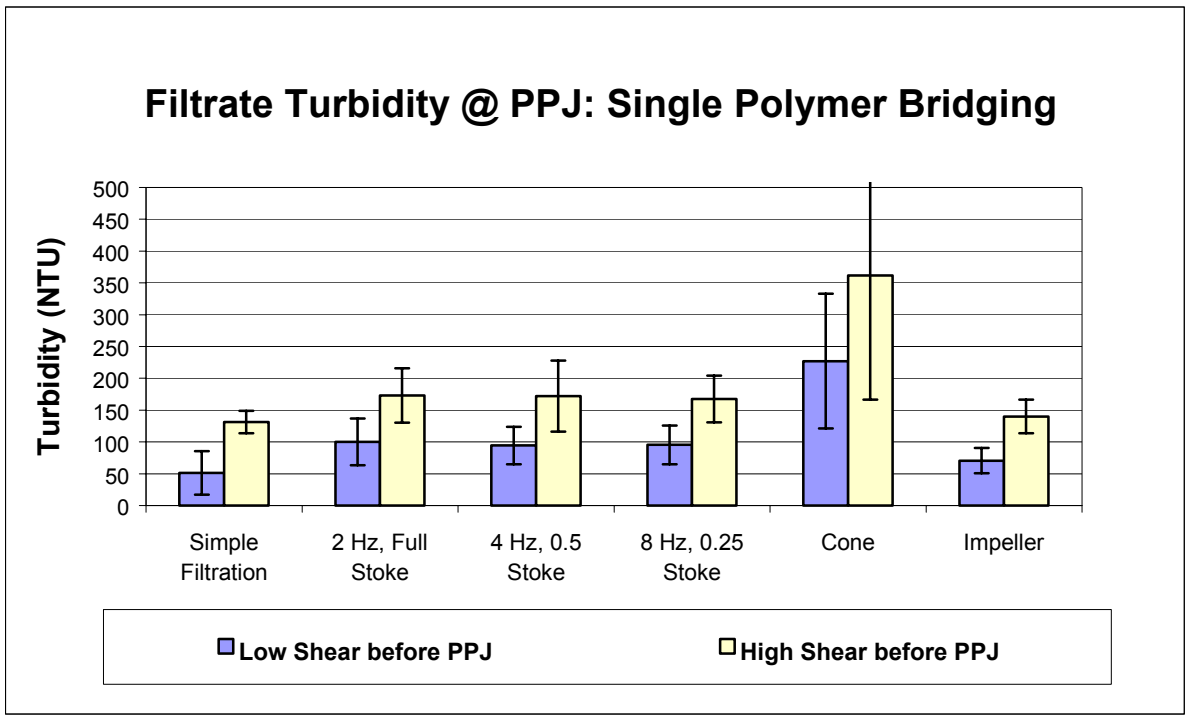

Figure 20 Turbidity results of different forming regimes (single polymer bridging)

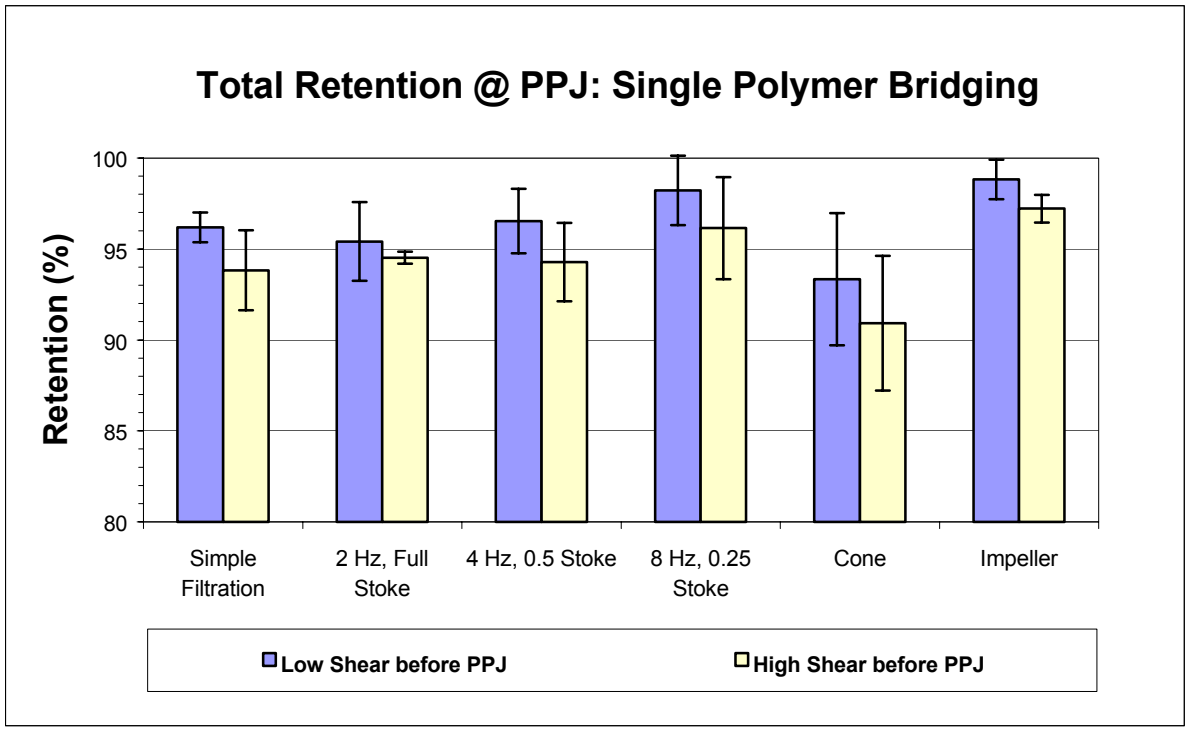

Figure 21 Total retention of different forming regimes (single polymer bridging)

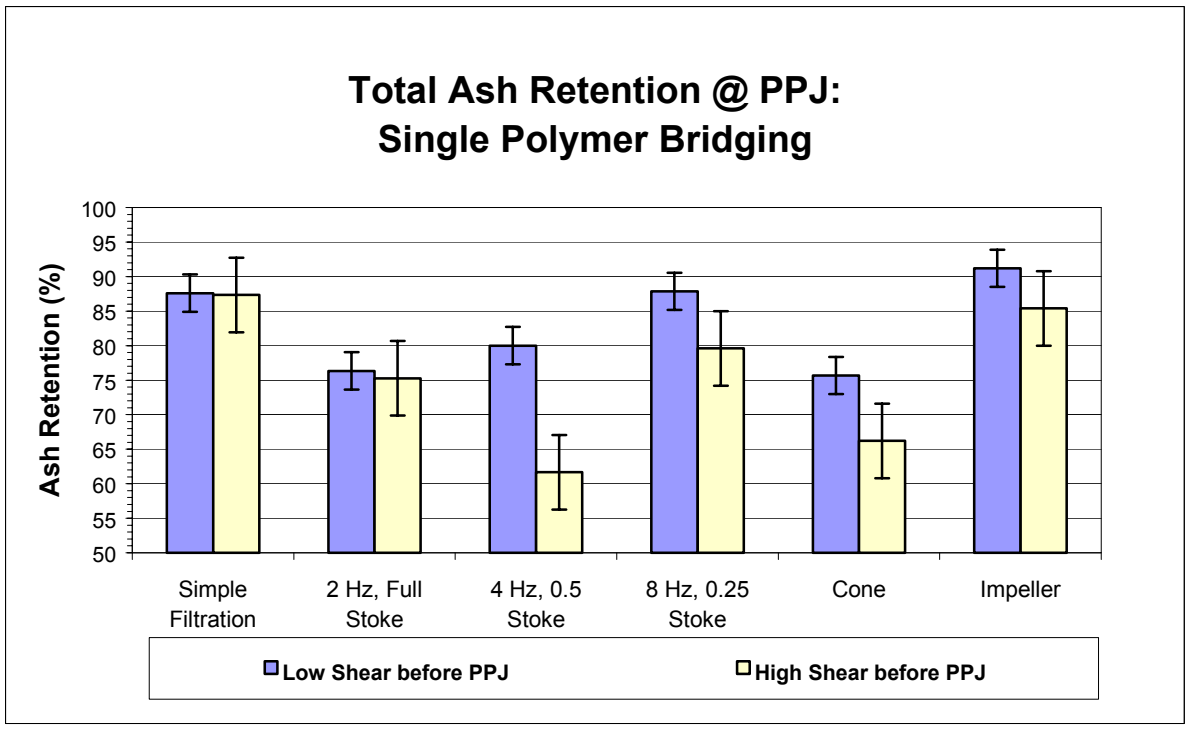

Figure 22 Total ash retention of different forming regimes (single polymer bridging)

Figures 20 to 22 show the results of single polymer bridging system. Results showed that the turbidity, total retention, and ash retention all showed the same trends resulting from different types of forming regimes. The cone stirrer showed the biggest effect of mat disruption compared with the others. Compared with the control set (Figure 16), the retention aid (cPAM) markedly decreased the filtrate turbidity, but no significant changes were found in total retention or ash retention. This may be due to the fact that most of the particles in the filtrate were the filler particles. These fillers would be expected to affect the turbidity measurement more than the fines did. So, it would be easier to observe changes based on turbidity tests, compared to retention tests. In addition, the pre-shear effects on single polymer systems were clearly observed. The high shear level increased the turbidity of filtrate and decreased the retention. This observation is consistent with the model that an increase of shear level created more breakage of polymer chains and these polymers could not reattach or flocculate again. These results are consistent with previous work (13,25,50).

Dual Polymer Bridging

In the dual polymer bridging system, the pulp slurries following the recipes in Table 1 were mixed with the Poly-DADMAC at a dosage of 0.20% on dry mass (200 rpm, 30 sec), followed by adding of aPAM at a dosage of 0.05% on dry mass and mixing (200 rpm, 30 sec). Different shear levels were applied to the pulp after mixing but before PPJ drainage. Different types of forming regimes on the PPJ were applied during formation of the mat in the case of those pulp slurries.

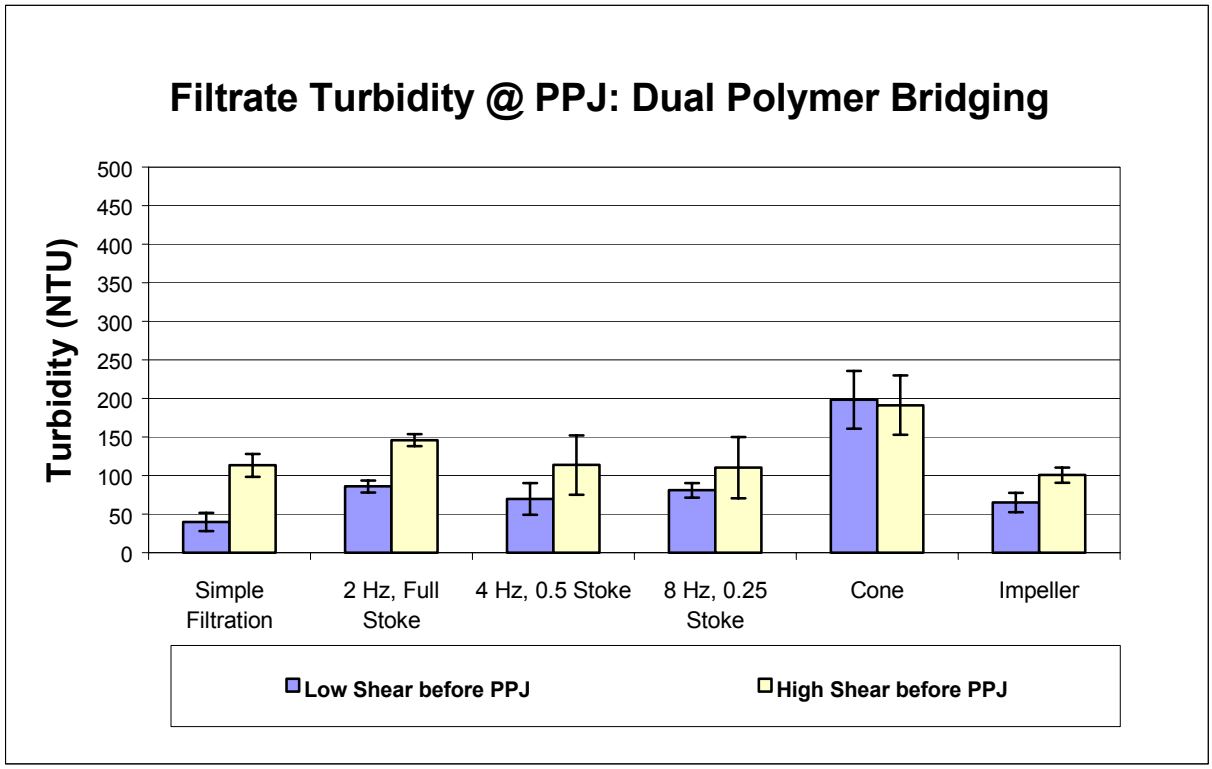

Figure 23 Turbidity results of different forming regimes (dual polymer bridging)

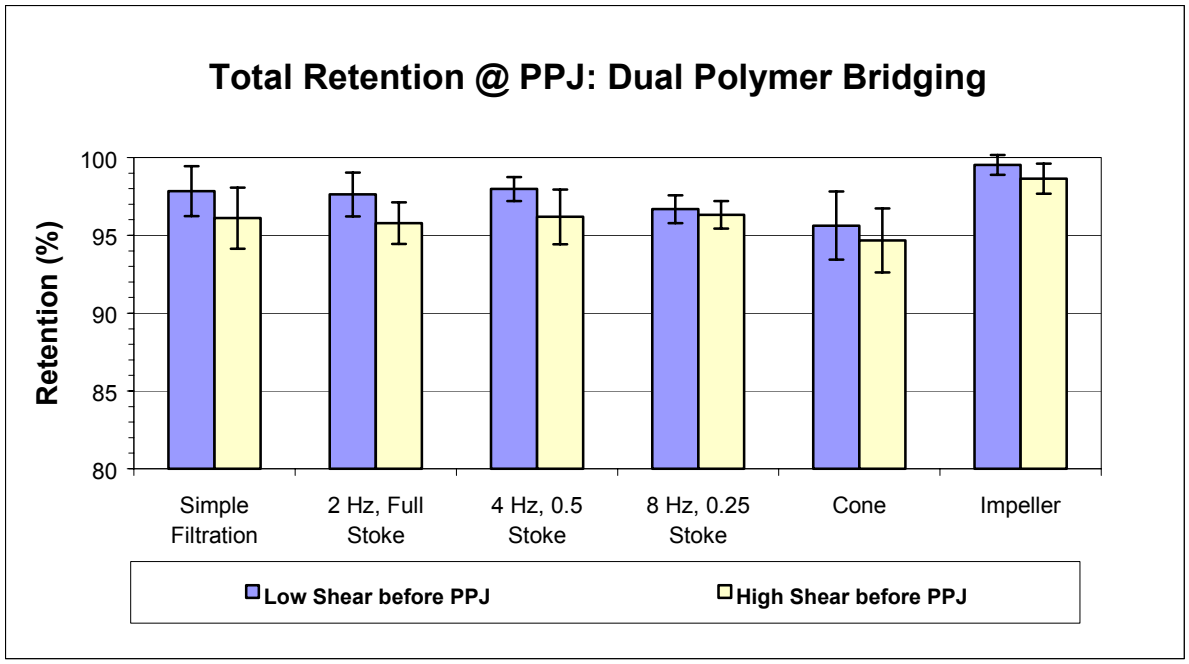

Figure 24 Total retention of different forming regimes (dual polymer bridging)

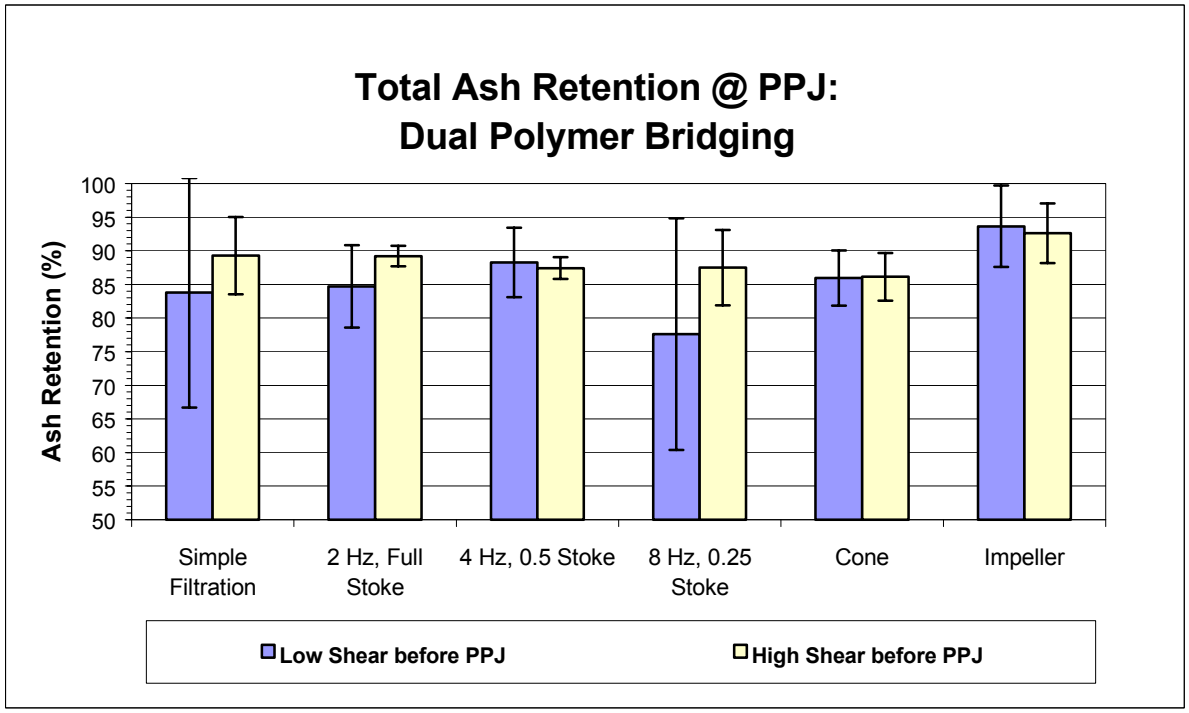

Figure 25 Total ash retention of different forming regimes (dual polymer bridging)

Figures 23 to 25 show the results of different forming regimes on a dual polymer bridging treatment (Poly-DADMAC & aPAM). Again, the turbidity, total retention, and ash retention showed the same trends resulting from different types of forming regimes as in single polymer system. Compared with the control set, the dual polymer system created more change in these parameters than the single polymer system did. It showed a greater decrease in filtrate turbidity than in the case of single polymer system. Moreover, the results corresponding to dual polymer treatment showed some trends in improvement of total retention that were not apparent in the case of single polymer treatment. These phenomena may be explained based on the fact that the dosage of Poly-DADMAC was double that of the dosage required for neutralization (Table 13). The excess Poly-DADMAC can be expected to help particle agglomeration both by itself and via a bridging mechanism. It also can be expected to have helped in reversibility of particle flocs through the mechanism of charge neutralization. These explanations were confirmed with the results of tests at different shear levels. The dual polymer system tended to create the stronger linkages than those in the single polymer system. These linkages also had stronger ability to resist the effect of shear force. Finally, these effects resulted in a narrower gap between the low shear domain and the high shear domain.

Charge Neutralization

In the charge neutralization system, the pulp slurries following the recipe in Table 1 were mixed with the Poly-DADMAC at a dosage of 0.20% on dry mass (200 rpm, 3 min). Different shear levels were applied to the pulp after mixing but before PPJ drainage. Different types of forming regimes on the PPJ were applied during formation of the mat in the case of those pulp slurries.

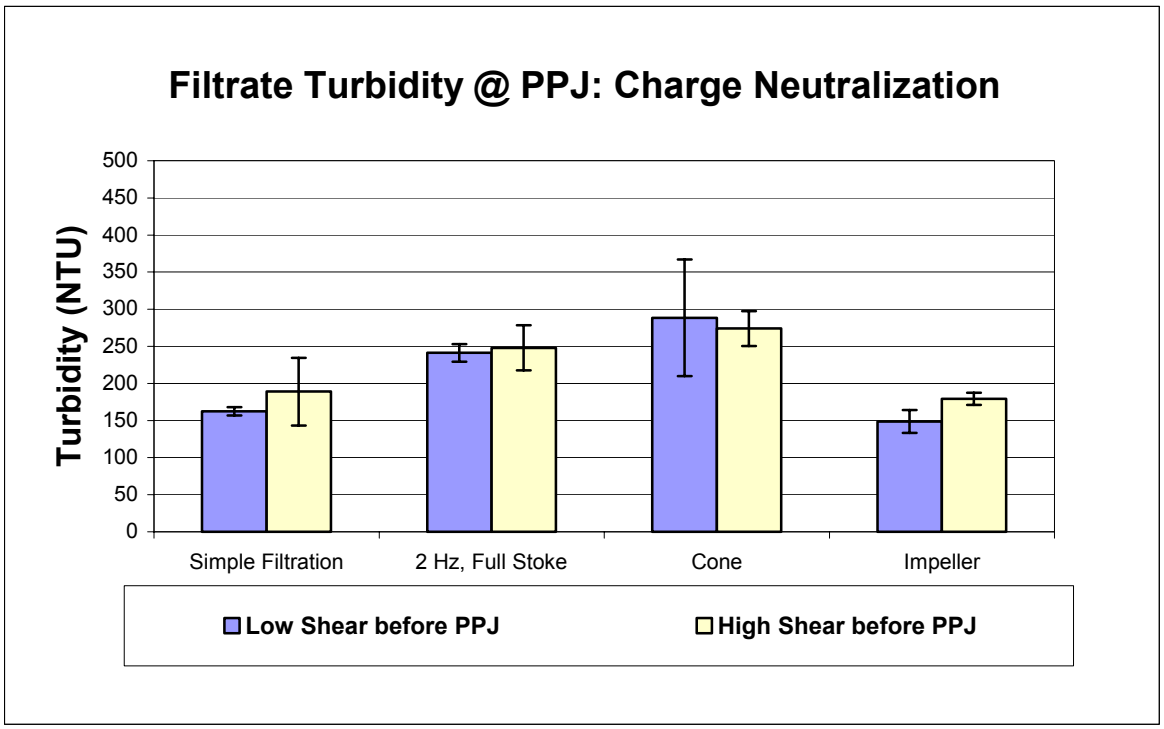

Figure 26 Turbidity results of different forming regimes (charge neutralization system)

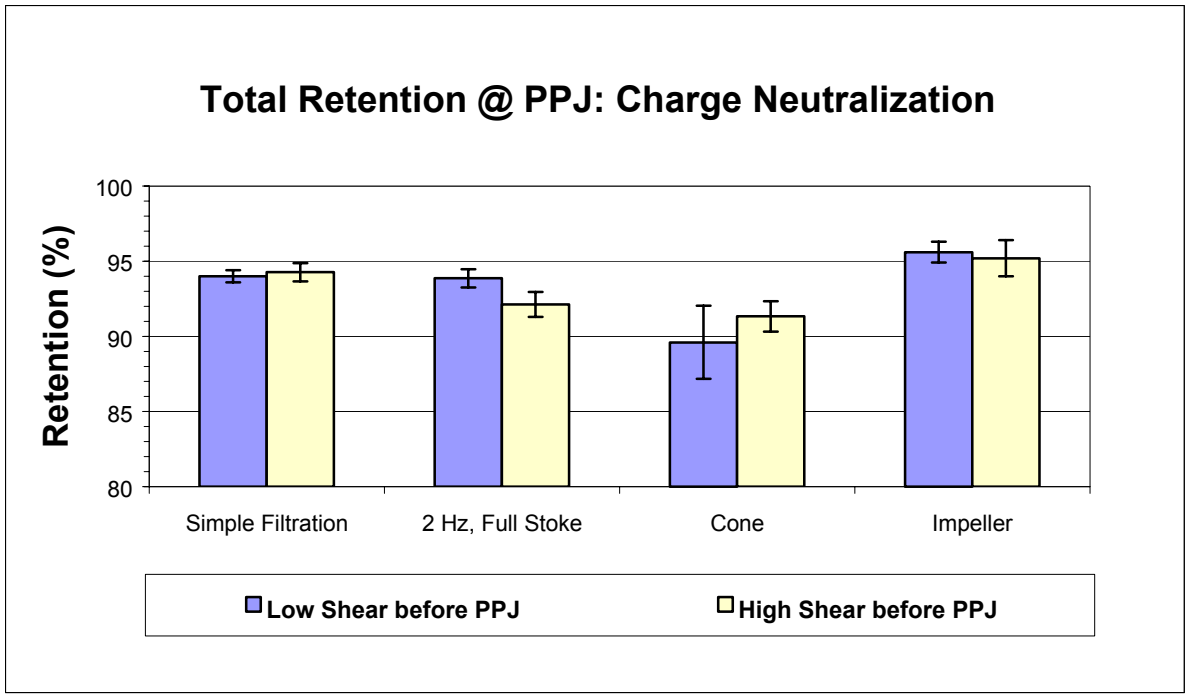

Figure 27 Total retention of different forming regimes (charge neutralization system)

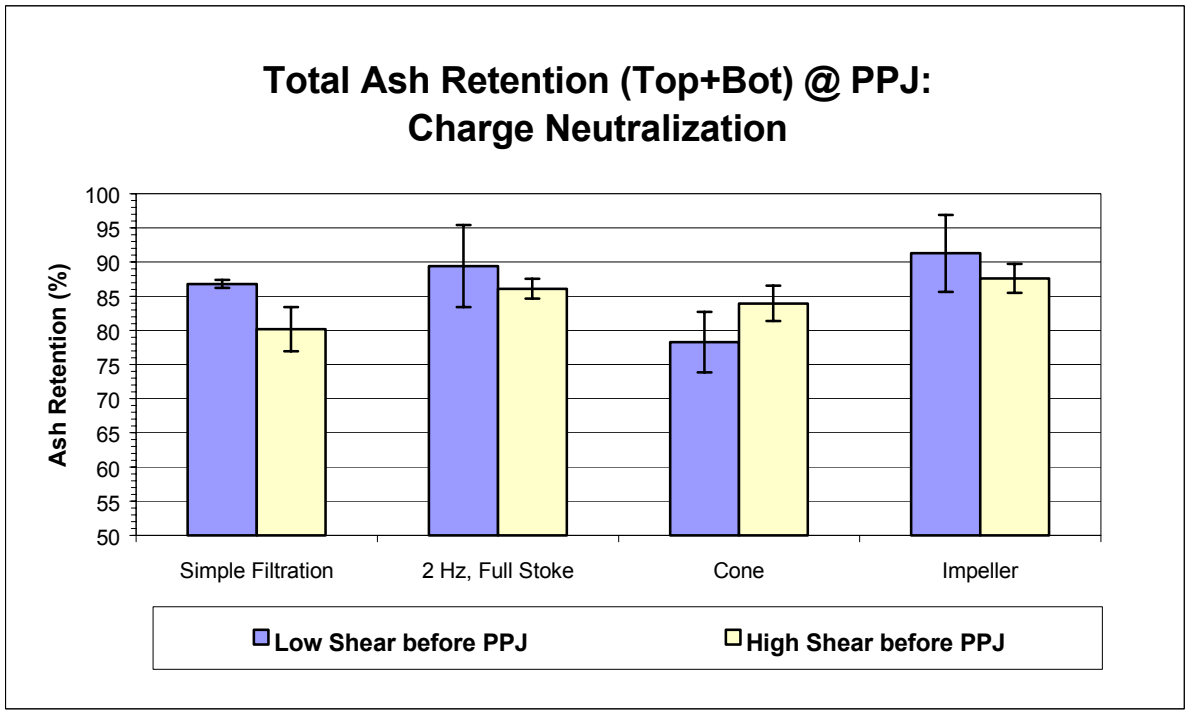

Figure 28 Total ash retention of different forming regimes (charge neutralization system)

Figures 26 to 28 show the results of charge neutralization under different forming regimes. The responses of the charge neutralization system showed the same trends as bridging polymers. The highest level of mat disruption came from the cone stirring. The simple filtration and the impeller stirring tended to give the same result. The selected pulsation level used in this set of tests (2 Hz & Full stroke) had effects that indicated less disruption of the fiber mat, compared to cone stirring. The interesting aspect from this series of experiments was the effect of pre-shearing. There is no specific information that would lead one to conclude that pre-shear conditions would affect this mechanism. The results of charge neutralization imply a reversible process. After exposure to the shear regimes, the particles can come closely and reattach together. Compared with the results corresponding to the bridging system, the charge neutralization condition performed worse than the bridging treatments with respect to retention, based on gravimetric and turbidity measurements. This may be due to the fact that the charge neutralization mechanism was dependent on weaker attractive forces. The particles couldn't reattach well during the forming processes especially the systems that have high level of hydrodynamic effects such as cone stirring and pulsation.

Charge Patch System

Figures 29 to 31 present the results due to pretreatment of the furnish samples with the charge patch additive recipe under different forming regimes. the pulp slurries following the recipe in Table 1 were mixed with the modified PEI at a dosage of 1.10% on dry mass (200 rpm, 3 min). Different shear levels were applied to the pulp after mixing but before PPJ drainage. Different types of forming regimes on the PPJ were applied during formation of the mat in the case of those pulp slurries.

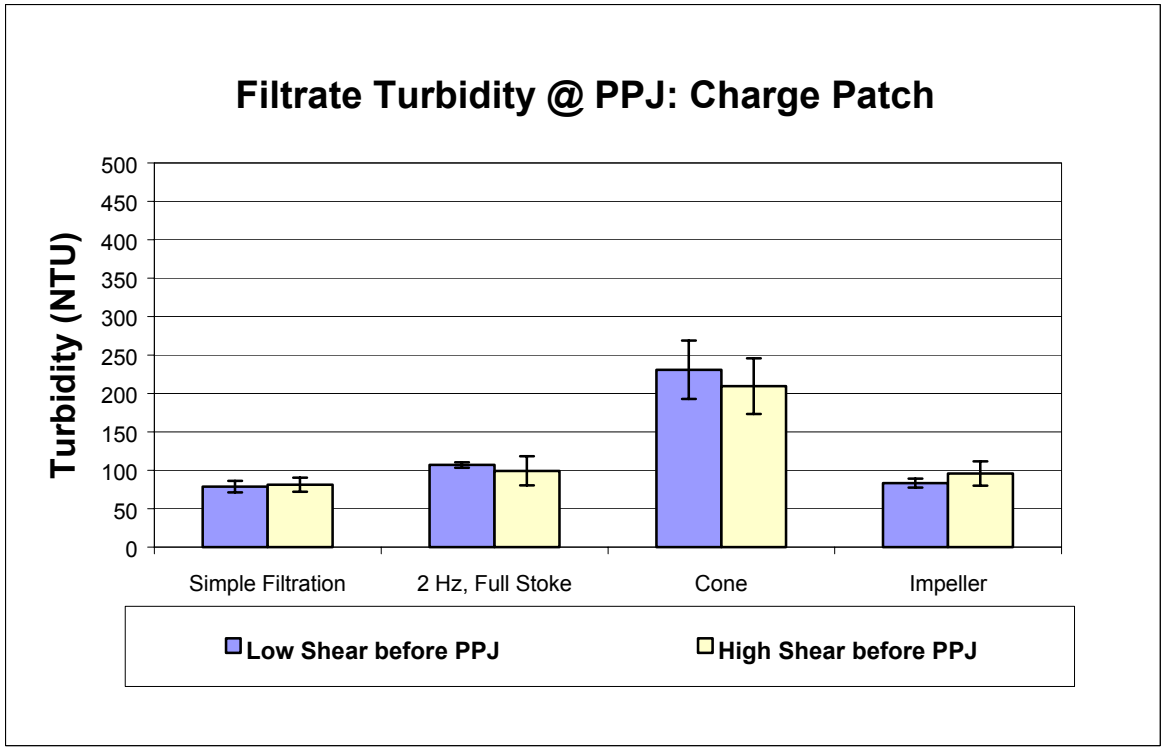

Figure 29 Turbidity results of different forming regimes (charge patch system)

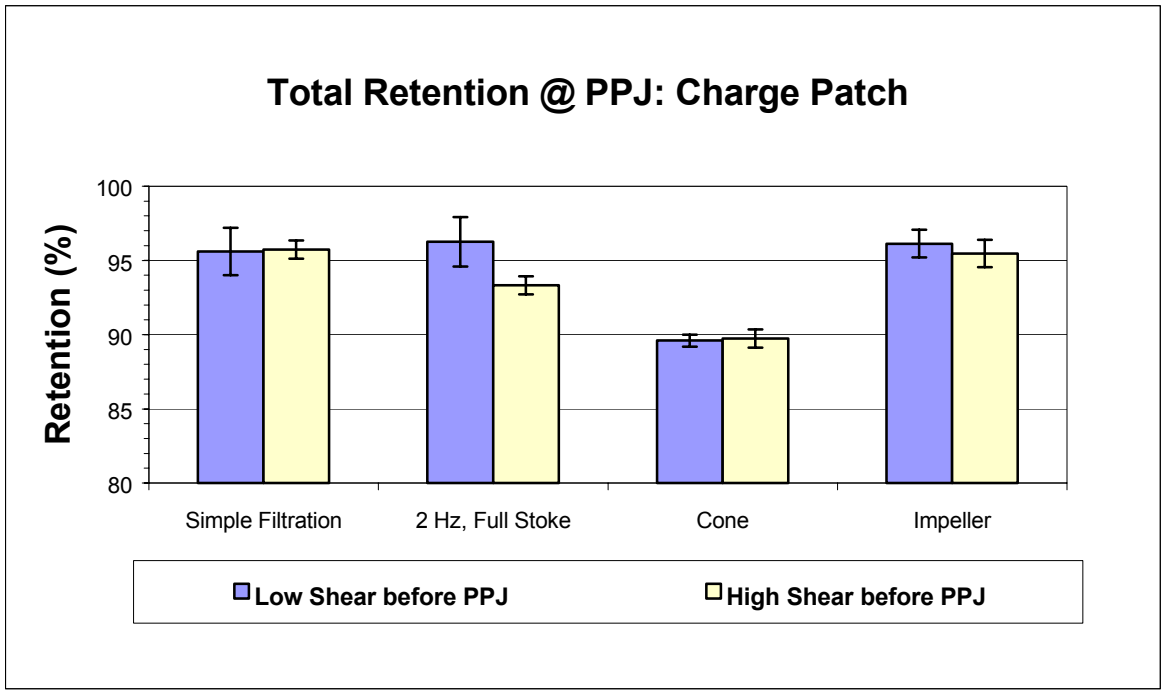

Figure 30 Total retention of different forming regimes (charge patch system)

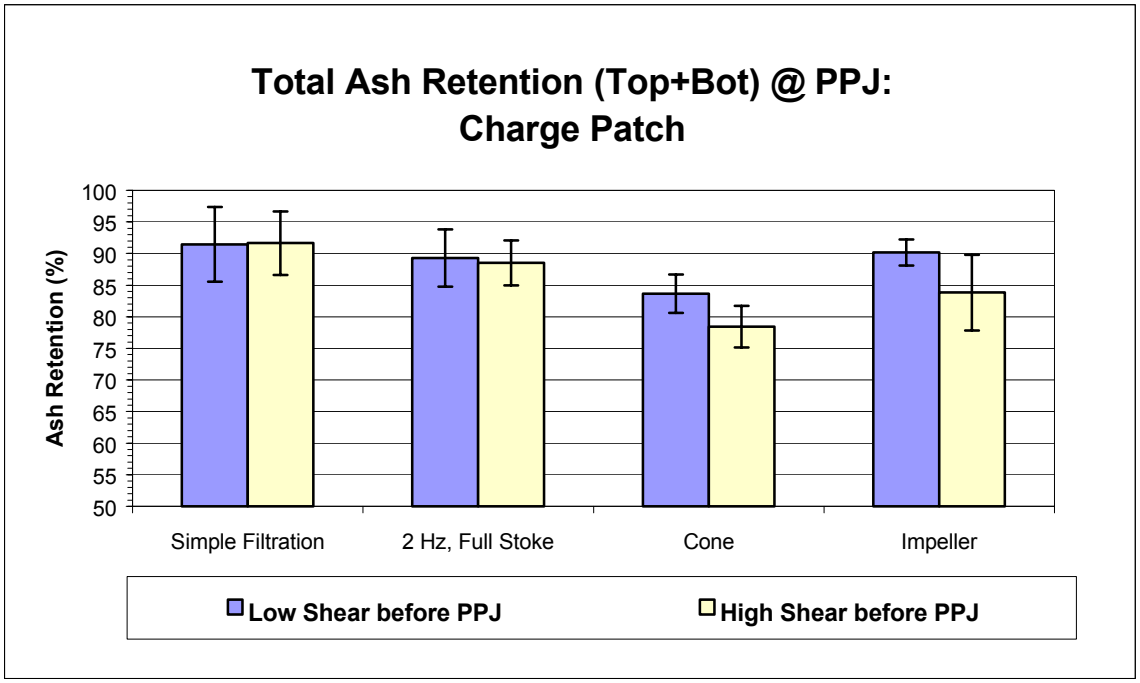

Figure 31 Total ash retention of different forming regimes (charge patch system)

Results in Figure 29 to 31 showed that different forming actions on the mat in the case of the charge patch treatment showed the same trends as in other systems. The turbidity was highest in the case of the cone stirring. Upon close inspection it is apparent that the charge patch system showed the same trends as in the case of charge neutralization. However, the improvements in retention and turbidity were greater. It was likely that the results from the low shear set were not significantly different from the results of the high shear set. A possible rationalization is that there was a reversible effect after shear exposure in each condition. However, the overall performance of the charge patch treatment was lower than the bridging system in every type of forming regime. A tentative explanation might be that the modified PEI lost its cationicity at the high pH. The pH value of this experiment was 9.1.

6.10 Responses of retention aid programs on simple filtration and pulsation

To understand the responses of different retention aid systems to simple filtration and pulsation (thickening effect) during dewatering, results were plotted in the form shown in Figures 32 and 33. These figures show the relative efficiency of different retention aids under each of the flow conditions considered. Filtrate turbidity was selected as the dependent variable. The pulsation in Figure 34 was set at the 2 Hz, full stroke condition.

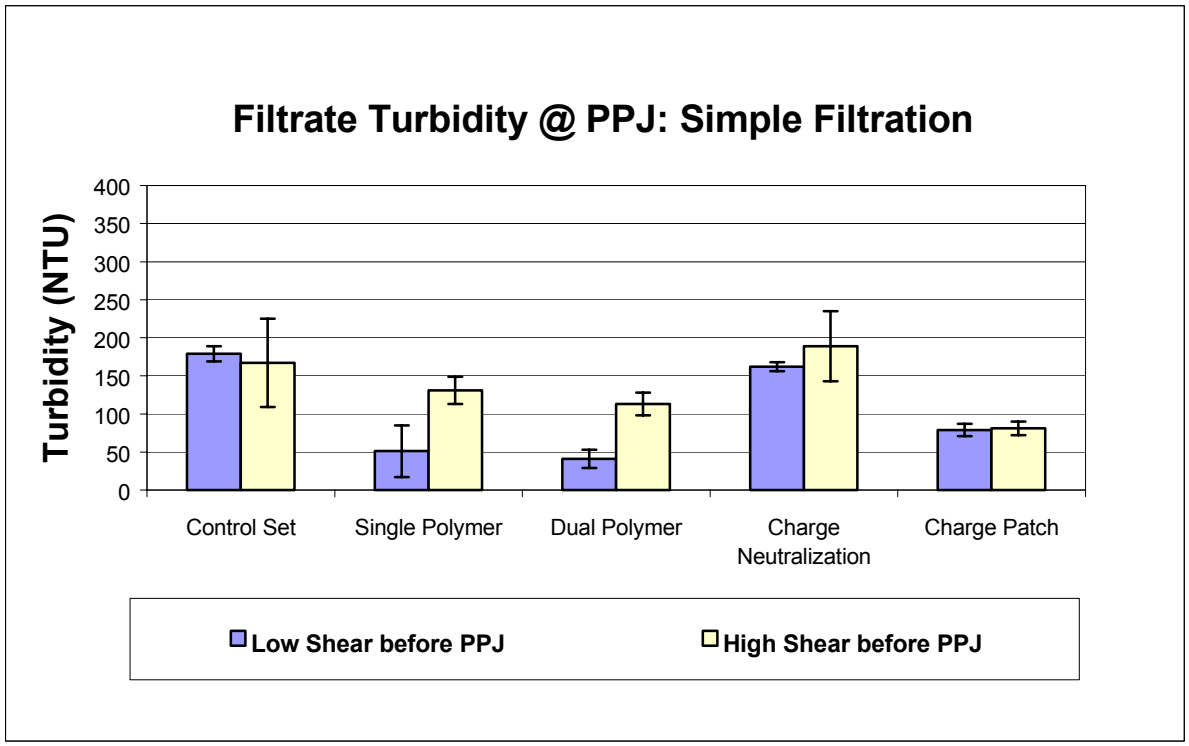

Figure 32 Turbidity results of different retention aid programs (simple filtration)

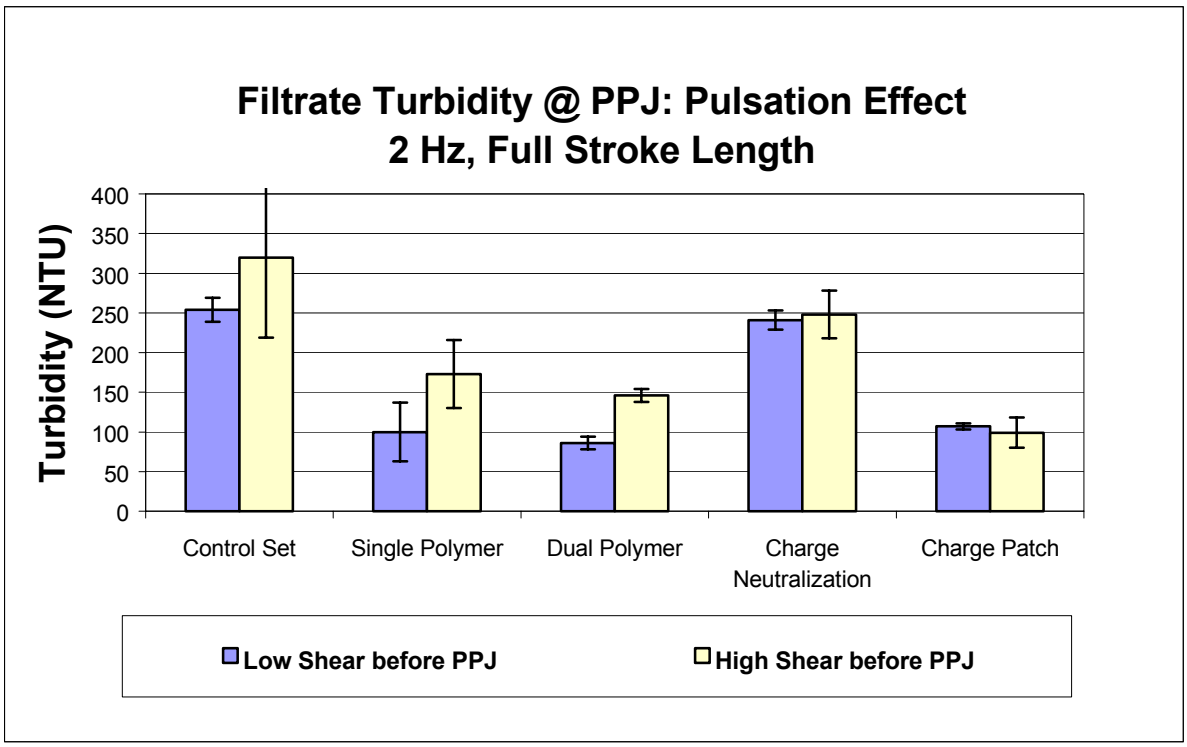

Figure 33 Turbidity of different retention aid programs (pulsation)

Figures 32 and 33 show the results that each regime had its own characteristic set of impacts on the mat, but that the levels of these effects were different in the effects of the different chemical treatment systems. Pulsation created more interruption on the mat and resulted in the higher value of turbidity, compared to simple filtration. In each of the forming regimes, retention aids improved the retention by reducing the turbidity. Dual polymer bridging seemed to be the most effective retention system, for reasons discussed in dual polymer bridging part of section 6.9. Again, charge neutralization and charge patch treatment showed reversible behavior, meaning that, according to the figures, different levels of pre-shearing had no significant effect on the subsequent results.

Figure 34 shows the relationship between filtrate turbidity values resulting from various chemical treatment conditions when comparing simple filtration and pulsation (2 Hz, full stroke). The diagram was plotted from the turbidity data in Figure 32 and Figure 33. The symbols represent the following conditions: the triangle marks refer to the control set; the circle marks represent the single polymer system; the square marks refer to the dual polymer system; the square with plus sign marks inside refer to the charge neutralization; and the diamond marks represent the charge patch system. The filled symbols refer to the low shear set and the unfilled symbols refer to the high shear set. The dash line represents the 45-degree line. Regardless of the type of retention aid systems and any level of shear before dewatering, the results showed a nearly linear relationship between the levels of filtrate turbidity resulting from simple filtration and pulsation. It appeared that the pulsation effect increased the filtrate turbidity in a proportional manner when compared with those in the simple filtration regime.

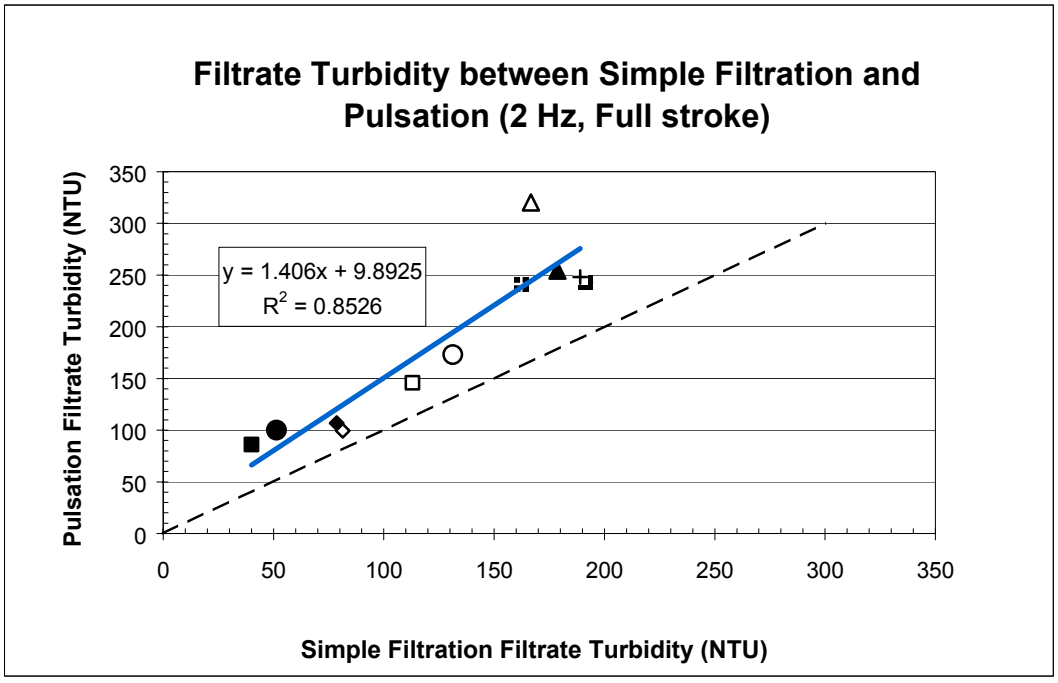

Figure 34 Relationship between simple filtration and pulsation effect in filtrate turbidity

7. CONCLUSIONS

1. The Positive Pulse Jar (PPJ) showed promising results for simulating idealized paper forming regimes such as simple filtration and pulsation-induced thickening.

2. Pulsation of flow perpendicular to the plane of the wet web was found to reduce the unevenness of fines and fillers in both x-y and z directions.

3. The amplitude of pulsation velocity perpendicular to the plane of the wet web can be calculated as a function of time with the Simple Harmonic Motion equation.

4. All of the retention aid systems that were studied decreased filtrate turbidity, indicating an effect on fine particle retention, especially filler retention.

5. Simple filtration, various frequencies and amplitudes of pulsating flow and uniform-shear regimes generally produced the same relative effects on each furnish system that had been pretreated with different types of retention aid program, though the different chemical systems showed different levels of susceptibility to shear.

6. Applied shear force and pulsation applied in this experiment could not completely destroy the positive effects of retention aid treatments on fines and filler retention.

7. In this study, the selected dual-polymer treatment system showed the most effective performance in reducing the filtrate turbidity when compared with other systems.

8. Charge neutralization showed the least-effective result when compared with other systems.

9. Pre-shearing at different levels before dewatering had a negative effect on the bridging systems.

10. Charge neutralization and charge patch treatments both showed reversible characteristics after the exposure of the fiber slurry to pre-shearing conditions.

8. PROPOSED FUTURE WORK

Although the work in this thesis was performed carefully in such a way as to compare the effects of different forming regimes, the results were not clear enough to determine the level of mat disruption quantitatively. The results from this thesis were mostly based on indirect measurement techniques such as turbidity, fines contents, and ash contents. The character of wet mat and drainage behaviors during the forming process in the PPJ experiments were not determined directly. It would be more precise to determine these effects at the same time with some electronic devices. Specific filtering resistance (SFR) measurement and pressure/vacuum electronic detectors could be some developments that could be included in a future version of the PPJ.

Another possibility is that the effect of different forming regimes could be identified in a common term or index based on some parameter. The term “mat disruption index” could be used in explaining the activity of the mat under different kinds of forming processes. Advanced statistical analysis would be an important tool in evaluating the effects of each parameter and predicting the relationships between those parameters. The activity of the mat influenced by some effect above the wire would be another idea in reducing the two-sideness problems of paper from Fourdrinier paper machine. A cone stirrer could play a role in simulating this effect during dewatering. Pulsation effects should be calibrated with the real action on the existing paper machine.

Studies of new retention aids systems in the future could also be done with PPJ device.

9. REFERENCES

1. Auhorn, W., "Web Formation, Drainage, and Drying Improved by Chemistry," *Wochenbl. Papierfabr. 110* (5): 155 (1982).

2. Wegner, T. H., Springer, A. M., and Chandrasekaran, S., "Single Procedure for Measuring Drainage, Retention, and Response to Vacuum of Pulp Slurries," *Tappi J. 67* (4): 124 (1984).

3. Cheng, Z., Saharinen, E., and Paulapura, H., "Laboratory Device (RPA) for Characterizing the Influence of Shear Forces on Retention, Part Two: Influence of High Shear Pulse," *Proc. Tappi Papermakers Conference*: 15 (1993).

4. Räisänen, K. O., Paulapura, H., and Karrila, S. J., "The Effects of Retention Aids, Drainage Conditions, and Pretreatment of Slurry on High-Vacuum Dewatering: a Laboratory Study," *Tappi J. 74* (4): 140 (1995).

5. Räisänen, K. O., Paulapura, H., and Karrila, S. J., "Wire Section Simulation with the Moving Belt Drainage Tester (MBDT)," *Proc. TAPPI 1993 Papermakers Conf.*: 103 (1993).

6. Persson, T., Osterberg, L., "A Laboratory Apparatus for Pulsed Drainage," *Svensk Papperstidning 72* (8): 446 (1969).

7. Britt, K. W., and Unbehend, J. E., "Water Removal during Sheet Formation," *Tappi 63* (4): 67 (1980).

8. Britt, K. W., and Unbehend, J. E., "Water Removal during Paper Formation," *Tappi J. 68* (4): 104 (1985).

9. Gess, J. M., "A New Drainage Analysis System," *Tappi J. 67* (3): 70 (1984).

10. Forsberg, S. and Bengtsson, M., "The Dynamic Drainage Analyzer (DDA)," *Proc. TAPPI 1990 Papermakers Conf.*: 239 (1990).

11. Sampson, W. W., "The Independence of Sheet Structure and Drainage," *Paper Technol. 38* (8): 45 (1997).

12. Attwood, B.W., and Jopson, R. N., "Dynamic Drainage Simulation," *Paper Technol. 39* (4): 53 (1998).

13. Neimo L., Ed., *Papermaking Chemistry*, Finish Paper Engineers' Association and Tappi, Finland, 1999.

14. Scott, W. E., *Principles of Wet End Chemistry*, TAPPI Press, Atlanta, 1996.

15. Gess, J. M., Ed., *Retention of Fines and Fillers during Papermaking*, TAPPI Press, 1998.

16. http://www.perplas.com/paper/dewater.htm

17. Ferguson, K., Ed., *New Trends & Developments in Papermaking*, Pulp & Paper Technical Insight Series, Miller Freeman Books, San Francisco, 1994.

18. Bell, N. E., "Optimal Forming Zone Design Is Key to Superior Sheet Characteristics," *New Trends & Developments in Papermaking*, Miller Freeman Books, San Francisco, 114 (1994).

19. Smook, G.A., *Handbook for Pulp and Paper technologists*, Second Ed., Angus Wilde, Vancouver, 1992.

20. Parker, J., *The Sheet Forming Process*, STAP No.9, TAPPI, Atlanta, 1972.

21. Paulapuro, H., *Paper and Board Grades*, Finish Paper Engineers' Association and Tappi, Finland, 2000.

22. Macabe, W. L., Smith, J. C., and Harriott, P., *Unit Operations of Chemical Engineering, 4th Ed.*, McGraw-Hill, Inc., New York, 1985.

23. Hubbe, M. A., *WPS 322 NCSU coursepack (Wet End Chemistry)*, Sir Speedy, Raleigh, 2001.

24. Niskanen K., Ed., *Paper Physics*, Finnish Paper Engineers' Association and Tappi, Finland, 1998.

25. Hubbe, M. A., *WPS 527 coursepack (Wet End Chemistry)*, Department of Wood and Paper Science, NCSU, Raleigh, 2001.

26. Heitmann, J. A., *WPS 261 NCSU course material (Papermaking Technology)*, Department of Wood and Paper Science, NCSU, Raleigh, 1999.

27. Unbehend, J. E., and Rowland, M. J., "Vacuum dewatering of hardwood and softwood pulps – role of wet mat compaction," SUNY College of environmental Science and Forestry, ESPRI Research Reports 81: VII: 86, 1996.

28. Wågberg, L., "A Device for Measuring the Kinetics of Flocculation Following Polymer Addition in Turbulent Fiber Suspensions," *Svensk Papperstidning 88* (6): R48 (1985).

29. Keiser, B. A., and Govoni, S. T., "Monitoring Flocculation of Newsprint in the Laboratory and on a Paper Machine," *TAPPI Papermakers Conf.* (2001).

30. Onabe, F., "Studies of Interfacial Phenomena Using the Colloid Titration Method," *I'Mokuzai Gakkaishi 28* (7): 437-444 (1982); Part 2, *28* (7): 445-451; Part 3, *29* (12): 900-908 (1983).

31. Sampson, W. W., Kropholler, H. W., "Batch-drainage curves for pulp characterization Part 1: Experimental", *Tappi J. 78* (12): 145 (1995).

32. Forsberg, S., and Bengtsson, M., "The Dynamic Drainage Analyzer (DDA)," *Proc. TAPPI 1990 Papermakers Conf.*, 239-245 (1990).

33. Gess, J. M., "Drainage/Retention Inter-relationships using the G/W System," *Proc. TAPPI 1983 Retention and Drainage Seminar,* 77 (1983).

34. Gess, J. M., "The Effect of Anionic Polymers and Mixing Time on the Drainage Characteristics of a Papermaking Pulp," *Proc. TAPPI 1993 Papermakers Conf.*, 79-85 (1993).

35. Saharinen, E., Cheng, Z., and Paulapuro, H., "Laboratory Device (RPA) for Characterizing the Influence of Shear Forces on Retention. Part One: Retention Process and Retention Index," *Proc. 10th Symp. The Chemistry of Papermaking,* Munich, Germany, Sept. 15-18, 1992.

36. http://www.brittjar.com

37. TAPPI Test Method T 261 cm-94, "Fines Fraction of Paper Stock by Wet Screening".

38. Penniman, J. G., *Dynamic Paper Chemistry Jar and Hand-Sheet Mold Operating Manual*, Paper Chemistry Laboratory, Inc., New York, 1986.

39. Britt, K. W., "Retention of Additives During Sheet Formation," *Tappi 56* (3): 83-86 (1973).

40. Britt, K. W., and Unbehend, J. E., "Monitoring Retention and Drainage on Paper Machines with the Dynamic Drainage Jar," *Seattle Retention and Drainage Aid Short Course*, 1977, pp. 46-49.

41. Avery, L. P., "Evaluation of Retention Aids. The Quantitative Alum Analysis of a Papermaking Furnish and the Effect of Alum on Retention," *Tappi 62* (2): 43-46 (1979).

42. Milliken, J. O., "Spectrophotometric Determination of Fines Retention Using the Dynamic Retention/Drainage Jar," *Seattle Retention and Drainage Short Course,* 1977, pp. 55-57.

43. Pelton, R. H., Allen, L. H., and Nugent, H. M., "A Survey of Potential Retention Aids for Newsprint Manufacture," *Proc. CPPA Ann. Mtg.,* Paper 213, B163, 1979.

44. Unbehend, J. E., "Mechanisms of "Soft" and "Hard" Floc Formation in Dynamic Retention Measurement," *Tappi 59* (10): 74-77 (1976).

45. Britt, K. W., and Unbehend, J. E., "Water Removal During Sheet Formation," *Tappi 63* (4): 67-70 (1980).

46. Britt, K. W., Unbehend, J. E., and Shridharan, R., "Observations on Water Removal in Papermaking," *Tappi J. 69* (7): 76 (1986).

47. Arslan, K., Bousfield, D. W., and Genco, J. M., "Effect of Shear Forces on Fine Particle Retention," *Tappi J. 80* (1): 254-261 (1997).

48. Au, C. O., and Thorn, I., Ed., *Applications of Wet-End Paper Chemistry*, Blackie Academic & Professional, London, 1995.

49. http://www4.ncsu.edu:8030/~hubbe/Defnitns/Bridging.htm

50. Roberts, J. C., Ed., *Paper Chemistry, 2nd Ed*., Blackie, London, 1996.

51. http://www4.ncsu.edu:8030/~hubbe/Defnitns/Neutrlzn.htm

52. Ström, G., and Kunnas, A., "The Effect of Cationic Polymers on the Water Retention Value of Various Pulps," *Nordic Pulp Paper Res. J. 6* (1): 12 (1991).

53. TAPPI Test Method T 200 om-89, "Laboratory Processing of Pulp (Beater Method)".

54. http://www4.ncsu.edu:8030/~hubbe/PAM.htm

55. http://www4.ncsu.edu:8030/~hubbe/DADM.htm

56. http://www4.ncsu.edu:8030/~hubbe/PEI.htm

57. http://www.pumpschool.com/principles/external.htm

58. http://water.usgs.gov/owg/FieldManual/Chapter6/6.7.html

59. Robertson, G., Olson, J., Allen, P., Chan, B., and Seth, R., "Measurement of fiber length, coarseness, and shape with the fiber quality analyzer," *Tappi J. 82* (10): 93 (1999).

60. Parker, J., and Mih, W. C., "A New Method for Sectioning and Analyzing Paper in the Transverse Direction," *Tappi J. 47* (5): 254 (1964).

61. TAPPI Test Method T 550 om-93, "Determination of Equilibrium Moisture in Pulp, Paper, and Paperboard for Chemical Analysis".

62. TAPPI Test Method T 211 om-93, “Ash in Wood, Pulp, Paper, and Paperboard: Combustion at 525 ^{o}C”.

63. OpTest Equipment Inc. Staff, *Fiber Quality Analyzer LDA96 Operating Manual*, OpTest Equipment Inc., Hawkesbury, ON, Canada, 1999.

64. Kocman, V., and Bruno, P. J., “Thermal Stability of Paper Fillers: A Strong Case for a Low Temperature Paper Ashing,” *Tappi J. 79* (3): 303 (1996).

65. Tam Doo, P. A., Kerekes, R., and Pelton, R., “Estimates of Maximum Hydrodynamic Shear Stresses on Fiber Surfaces in Papermaking,” *J. Pulp Paper Sci. 10* (4): J80 (1984).

Appendices

10. APPENDICES

The following items are included in this Appendix.

- Appendix A – Beating curve
- Appendix B – Fractionation effect
- Appendix C – Bellows size selection
- Appendix D – Evaluation of FQA procedure
- Appendix E – Pulsation equation

Appendix A - Beating Curve

Objectives: To determine the beating time at level of 400 ml CSF for bleached hardwood kraft pulp (market pulp)

Equipment: Valley Beater

Procedures: TAPPI Method T-200

Results: Eighteen minutes is the beating time for the initial hardwood kraft pulp to have 400 ml CSF in freeness.

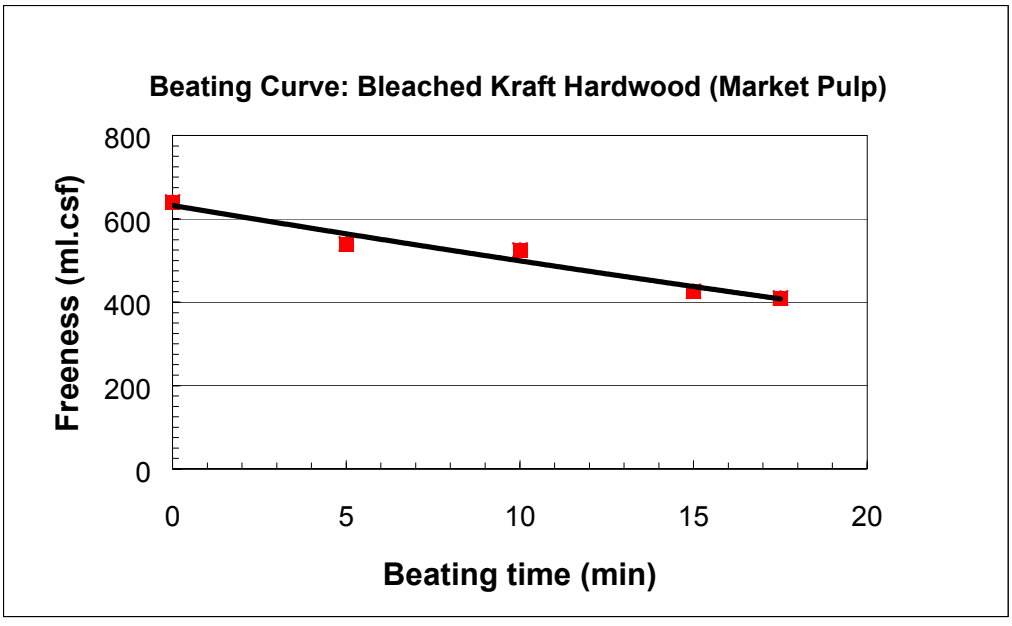

Appendix B - Fractionation effect

Objectives: To separate the fine particles from the refined pulp

Equipment: Bauer-McNett fractionator

Procedures: Operate Bauer-McNett fractionator at the water flow rate 1.2-1.5 liter/minute. Pour 2 liters of the refined pulp from Valley Beater to the 200-mesh slot of the fractionator. Pour another 2 liters of refined pulp into fractionator every 5 minutes. Stop and collect the fiber fraction after every 1-hour of fractionation. After finishing the 1^{st} pass of fractionation, redo the 2^{nd} pass of fractionation with the 1^{st} collected fiber fraction. Keep the filtrate from both passes into the barrel tank a night for sedimentation. Measure the fines content with FQA.

Results: Fines content in pulp decreased with the number of pass in fractionation. Freeness of the refined pulp increased after removal of the fines. The fiber length test showed the trend of fiber increase in the fiber fraction. After the 2^{nd} pass, the fiber fraction still has the amount of fines at 26% approximately. (based on the number of particles)

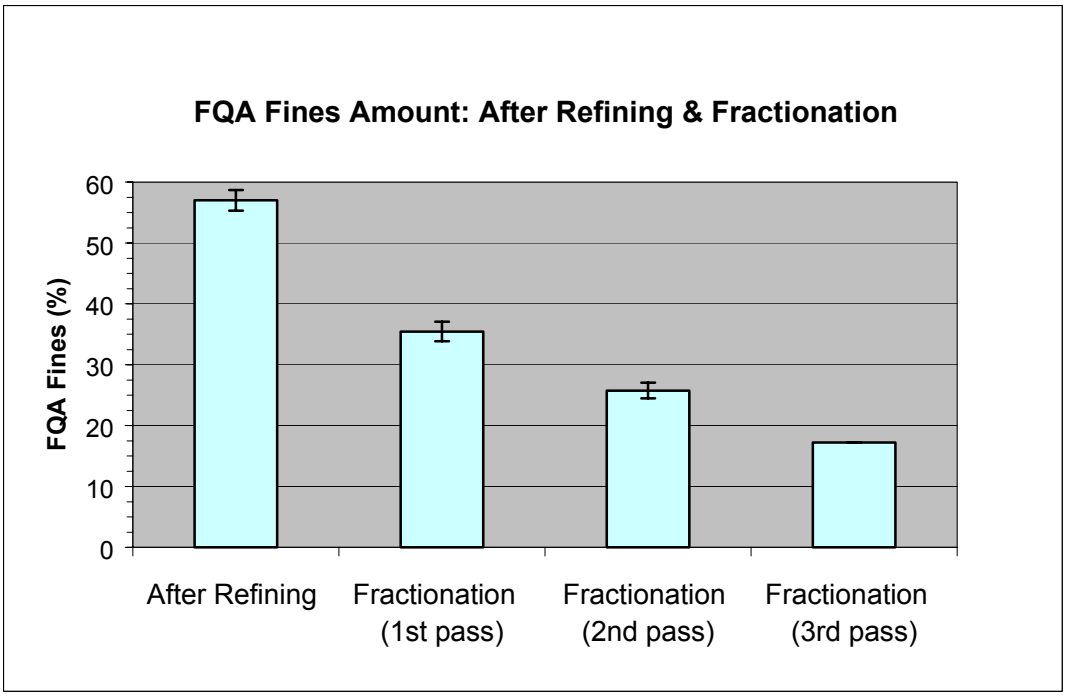
FQA Fines Amount: After Refining & Fractionation
FQA Fines (%)
60
50
40
30
20
10
0
After Refining
Fractionation (1st pass)
Fractionation (2nd pass)
Fractionation (3rd pass)

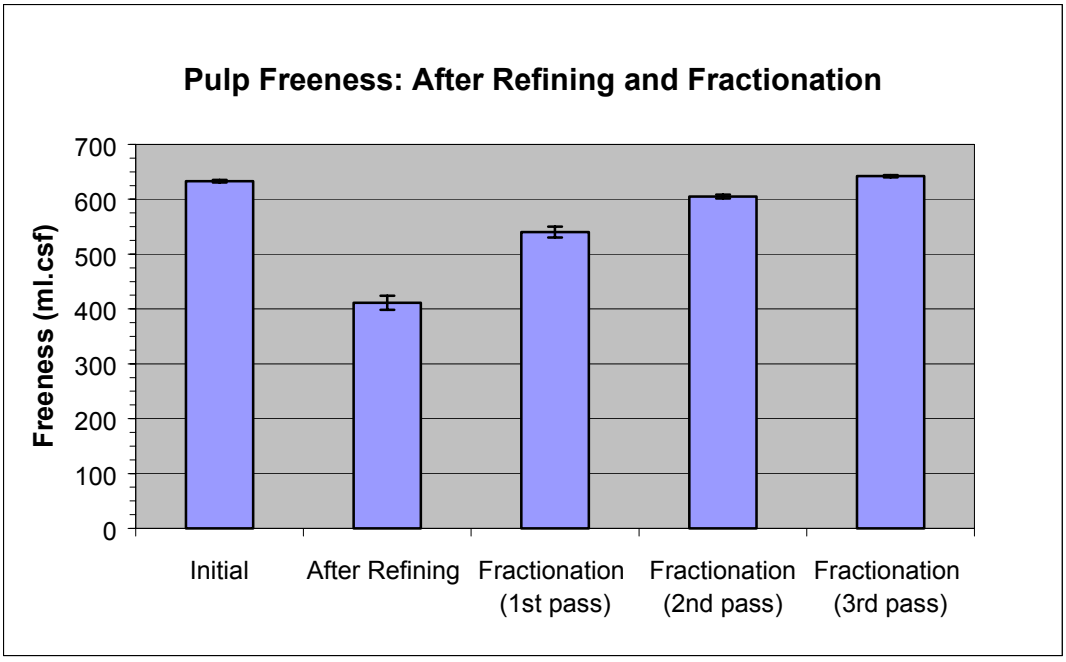
Pulp Freeness: After Refining and Fractionation
Freeness (ml.csf)
700
600
500
400
300
200
100
0
Initial
After Refining
Fractionation (1st pass)
Fractionation (2nd pass)
Fractionation (3rd pass)

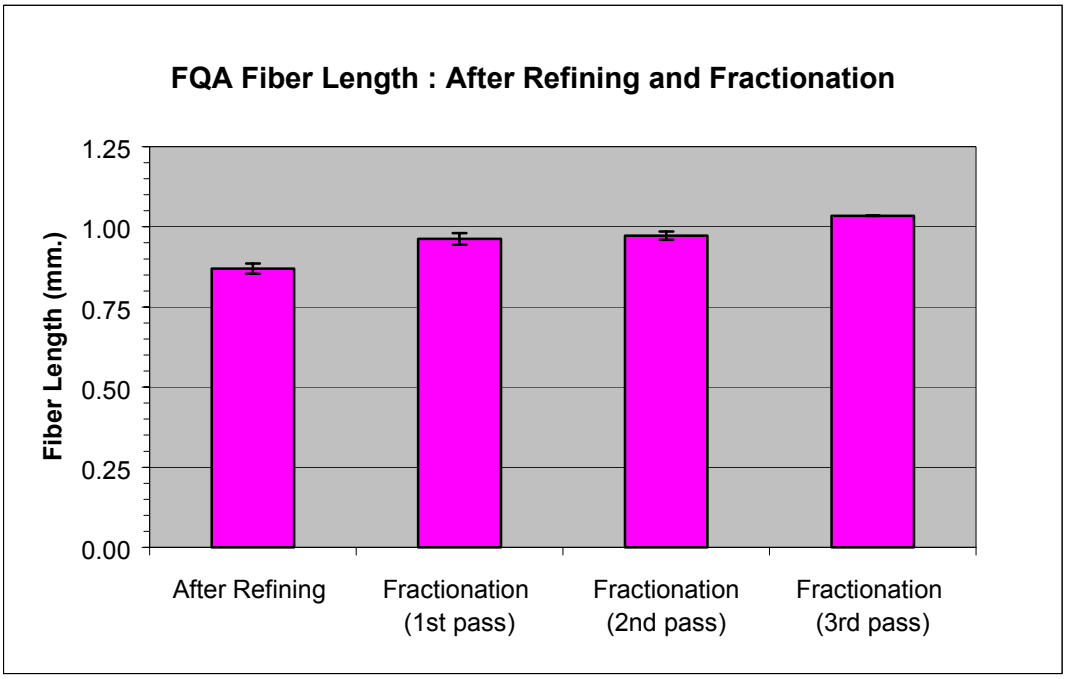

Appendix C - Bellow size selection

Objectives: To select the appropriate size of bellows that gives the appropriate pulsation effect for PPJ experiments

Equipment: Positive Pulse Jar device

Procedures: Operate PPJ with two types of pulp slurry; Bleached kraft pulp furnish and Newsprint furnish at different sizes of bellow (0.5, 1.0 and 1.5 inch in diameter)

Results: the medium bellow (1.0 inch in diameter) showed the maximum effect of pulsation with the turbidity measurement.

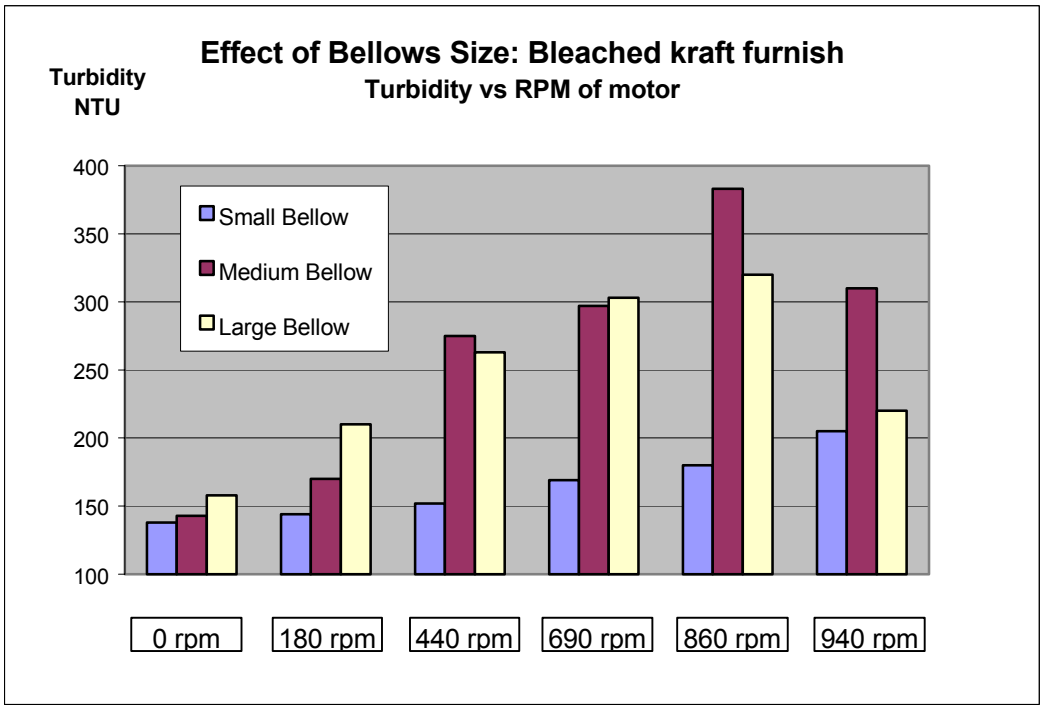
Effect of Bellows Size: Bleached kraft furnish
Turbidity vs RPM of motor
Turbidity NTU
400
350
300
250
200
150
100
Small Bellow
Medium Bellow
Large Bellow
0 rpm
180 rpm
440 rpm
690 rpm
860 rpm
940 rpm

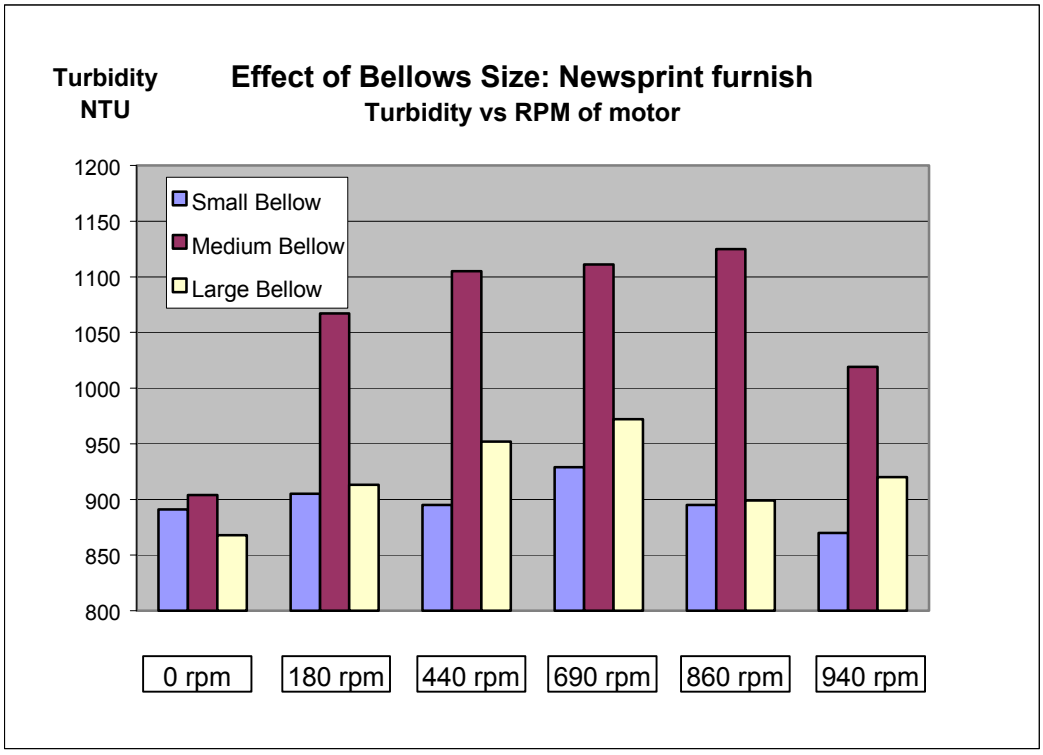
Effect of Bellows Size: Newsprint furnish
Turbidity vs RPM of motor
Turbidity NTU
1200
1150
1100
1050
1000
950
900
850
800
Small Bellow
Medium Bellow
Large Bellow
0 rpm
180 rpm
440 rpm
690 rpm
860 rpm
940 rpm

Appendix D - Evaluation of FQA Procedure

Objectives: To evaluate the fine-particle size determination of FQA and determine whether the results were sensitive to the presence of mineral filler

Equipment: Fiber Quality Analyzer

Procedures: Measure the FQA fines content with different %solid of filler slurry (5, 10 and 15 %)

Results: FQA didn't consider the filler particle in their analysis of fines content.

FQA Analysis of filler particle at different %solid

Filler	Fiber count	Fiber frequency,eps	Fiber length, mm	% Fine
5% solid	402	2.33	0.12	98.26
10% solid	2859	7.33	0.10	99.16
15% solid	919	3.33	0.33	95.32

Appendix E – Pulsation equation

Objectives: To find the predictive equation related to the pulsation actions in PPJ

Calculation basis: PPJ inside diameter 3.969 in., Plastic hose inside diameter 0.246 in., Gear pump flow rate = 26.41 cm^3/sec (Table 8), Observed difference of water level height was 9 in. or 22.86 cm. (from Figure 14 @ 0.42 Hz, Full Stroke). The reason for selecting the lowest frequency range of bellows pump action is to minimize inertial effects.

Gear pump velocity contribution = Volumetric rate / Screen area

Gear pump volumetric rate = 26.41 cm^3/sec

Screen area = $(\pi/4)$(Inside diameter of PPJ)^2 = $(\pi/4)(3.969*2.54)^2$

= 79.85 cm^2

So, Gear pump velocity contribution = (26.41 cm^3/sec) / (79.85 cm^2)

= 0.331 cm/sec

Amplitude of bellows pump = Volume of bellows / (2 * Screen area)

The volume of the bellows can be calculated from the change of water level in the plastic hose in Figure 14.

Volume of bellows = $(\pi/4)$(Inside diameter of plastic hose)^2 * h

= $(\pi/4)(0.246*2.54)^2 * 22.86$ = 7.012 cm^3

So, Amplitude = 7.012 cm^3 / (2*79.85 cm^2) = 0.0439 cm.

Simple harmonic equation of flow velocity in PPJ:

Velocity in PPJ = Amplitude*Stroke length fraction*$(2\pi f)[\text{Cos}(2\pi ft)]$ – Gear pump velocity contribution

$$\boldsymbol{V = 0.0439\, X_{SL}\, (2\pi f)[\text{Cos}(2\pi ft)] - 0.331}$$

V = Velocity, cm/sec

X_{SL} = Fraction of full stroke length (0 to 1), Figure 14

f = Frequency, Hz

t = Time, sec

For example: 2 Hz, Full stroke implies that

Max = +0.552 - 0.331 cm/sec = + 0.221 cm/sec

Min = -0.552 - 0.331 cm/sec = -0.883 cm/sec